Coupled ocean-atmosphere summer heatwaves in the New Zealand region: an update

M James Salinger[1], Howard J Diamond[2], James Bell[3], Erik Behrens[4], B Blair Fitzharris[5], Nicholas Herod[6], Melissa McLuskie[7], Amber K Parker[8], Hiltrun Ratz[9], James Renwick[1], Claire Scofield[10], Nick T Shears[11], Robert O Smith[12], Phil J Sutton[4] and Michael C T Trought[13]

[1] Department of Geography, Environment and Earth Sciences, Victoria University of Wellington, Wellington, New Zealand
[2] NOAA/Air Resources Laboratory, College Park, Maryland 20740, USA
[3] School of Biological Sciences, Victoria University of Wellington, New Zealand
[4] National Institute of Water and Atmospheric Research (NIWA), Wellington, New Zealand
[5] Department of Geography, University of Otago, Dunedin, New Zealand
[6] Applied Science Pty Ltd., Adelaide, Australia
[7] Western Bay Wildlife Trust, Tauranga, New Zealand
[8] Department of Wine, Food and Molecular Biosciences, Lincoln University, New Zealand
[9] Penguin Rescue, Moeraki Lighthouse, RD2 Palmerston, Otago, New Zealand
[10] New Zealand Institute for Plant and Food Research Limited, New Zealand
[11] Leigh Marine Laboratory, Institute of Marine Science, University of Auckland, New Zealand
[12] Department of Marine Science, University of Otago, Dunedin, New Zealand
[13] Innovative Winegrowing, Blenheim, New Zealand
Corresponding author: M. James Salinger, jimbosalinger09@gmail.com

KEY WORDS
Anthropogenic global warming, marine heatwave, atmospheric heatwave, terrestrial ecosystems, marine ecosystems, grapes

ABSTRACT

During austral warm seasons (November - March, NDJFM) of 1934/35, 2017/18, 2018/19 and 2021/22 the New Zealand (NZ) region experienced the most intense coupled ocean/atmosphere (MHW/AHW) heatwaves on record. Average temperature anomalies over land and sea were +1.2 to 1.4°C above average. Common to all four events were maximum sea surface temperature (SST) anomalies to the west of the South Island of NZ. Atmospheric circulation anomalies showed a pattern of blocking high pressure over the Tasman Sea and Pacific Ocean to the south, and southeast of NZ, and reduced trough activity over and to the east of NZ, accompanied by strongly positive Southern Annular Mode conditions.

Hindcasts for 2017/18, 2018/19 and 2021/22 NDJFM indicate that positive temperature anomalies around 1°C occurred in the Tasman Sea, and near 1.5°C for the Chatham Rise. The temperature anomalies in the upper 50m of the ocean are consistent with the 500hPa atmospheric height anomalies. The temperature anomalies in the upper 50m of the ocean are consistent with the 500hPa atmospheric height anomalies and associated winds. The eastern Tasman Sea during August 2021 to July 2022 experienced the highest annual number of MHW days during the satellite-era (1981-present) from OISSTv2.1 data. Under 1.5°C of global warming the four events would have ERIs of 2-3 years, and with 2°C of warming all would be considered cool years relative to the +2°C climate. For the 1957-2022 period, the two most intense heatwaves have ERIs of between 30 to 150 years.

Major loss of glacial ice occurred from Southern Alps glaciers with rapid melt of seasonal snow in all cases. Slow advances in grape phenology since 1948 may be associated with increases in temperature over the same period. Cherries and apricot harvest dates advanced by one to two weeks. Marine impacts may be linked to starvation of kororā/Little Penguin (*Eudyptula minor*) chicks in the Bay of Plenty. Chicks weighed less and had a lower body condition score in 2020 and 2021 compared to 2019 and rescue calls in 2021 reached the highest volumes since 2015. The first record of warm-water prey species in the diet of yellow-eyed penguins at Moeraki occurred, as well as widespread sea-sponge bleaching around northern and southern NZ.

1. INTRODUCTION

Yet another unparalleled heatwave occurred during the austral summer of 2021/22 in the New Zealand region. This followed a very warm summer in 2018/19, although not as intense as the 1934/35 or 2017/18 events. Salinger et al (2020) reviewed the characteristics of the three warmest austral summers (DJF) in the NZ region (approximately 4 million km^2) of 1934/35, 2017/18 and 2018/19. These summers experienced the most intense coupled ocean-atmosphere heatwaves on record.

Kidson (1935) described the first documented austral summer (DJF) heatwave covering the New Zealand (NZ) area in 1934/35, with regional temperatures anomalies over land averaging +1.7ºC compared to the 1981-2010 normal. At the time this event was so unusual, almost 3ºC warmer than other 1930s summers, it was described as "remarkably warm". Salinger et al (2019a) documented the unprecedented austral summer (DJF) 2017/18 heatwave covering the NZ region. Regional average air (over land) and sea surface temperature (SST) anomalies were +2.2ºC and +1.9ºC, respectively. Terrestrial and marine impacts that may be linked to the coupled atmosphere/marine heatwave (AHW/MHW) persisted for the entire austral summer resulting in (1) the largest loss of glacier ice in the Southern Alps since 1962; (2) early Sauvignon blanc wine-grape maturation; and (3) species disruption in marine ecosystems. The effects on marine ecosystems considered here included mortality of inshore low trophic level species, and distribution of pelagic species.

Average air temperature anomalies over land were +1.7 to 2.1°C while SSTs were 1.2 to 1.9°C above average. All three earlier heatwaves exhibited maximum SST anomalies west of the South Island of NZ. Atmospheric circulation anomalies showed a pattern of blocking high pressure centred over the Tasman Sea extending southeast of NZ, accompanied by strongly positive Southern Annular Mode conditions, and reduced trough activity over NZ. Rapid melt of seasonal snow occurred in all three cases.

For the 2017/18 and 2018/19 events, combined ice loss in the Southern Alps was estimated at 7.0km^3 water equivalents (22% of the 2017 volume). Sauvignon blanc and Pinot noir wine grapes had above average berry number and bunch mass in 2018 but were below average in 2019. Summer fruit harvest (cherries and apricots) were 14 and 2 days ahead of normal respectively. Spring wheat simulations suggested earlier flowering and lower grain yields compared to average, and below-average yield and tuber quality in potatoes crops occurred. Major species disruption occurred in marine ecosystems. Hindcasts indicate the heatwaves were either atmospherically driven or arose from combinations of atmospheric surface warming and oceanic heat advection.

Using the Hobday et al (2016) definition of MHW[1], Oliver et al (2018) found a 54% increase in the number of MHW days globally since the early 20th century with an increase of 3-9 days per decade in the NZ region. From two General Circulation Model (GCM) ensembles, Perkins-Kirkpatrick et al (2019) and Oliver et al (2017) concluded that a Tasman Sea MHW with the intensity of the 2017/18 event would have been virtually impossible without anthropogenic warming. However, the 1934/35 AHW/MHW stands out as an exception to this conclusion. The atmospheric blocking that was responsible for the prolonged period of high mean sea level pressure (MSLP) also displayed some anthropogenic influence, although Perkins-Kirkpatrick et al (2018) note that this detected influence was less than that on the sea surface temperature.

[1] A MHW is defined as a prolonged discrete anomalously warm water event that can be described by its duration, intensity, rate of evolution, and spatial extent. Specifically, an anomalously warm event is considered to be a MHW if it lasts for five or more days, with temperatures warmer than the 90th percentile based on a 30-year historical baseline period.

MHWs are caused by a range of processes at different spatial and temporal scales, from localised air–sea heat flux to large-scale climate drivers such as the El Niño/Southern Oscillation (ENSO; Heidemann and Ribbe, 2019) and Southern Annular Mode (SAM; Thompson et al., 2011). Behrens et al (2019) investigated mechanisms of MHWs in the Tasman Sea using a forced global ocean sea-ice model and Argo[2] observations, concluding that they are largely modulated by meridional heat transport from the subtropics through the interchange between the East Australian Current and the Tasman Front. One contributor to the increased frequency of MHWs (Oliver et al., 2018) has been regional warming trends. Sutton and Bowen (2019) documented a 0.1 to 0.3°C per decade increase in ocean temperatures since 1981 with warming penetrating from the surface to 200m depth around coastal NZ and to at least 850m in the eastern Tasman Sea. Ocean/atmosphere diagnostics from SSTs, mean sea level pressure (MSLP) and 500hPa geopotential height anomalies shows that these are coupled over the NZ region (Salinger et al., 2020).

Previous MHWs in the NZ region have been reported to have a number of impacts on marine organisms and primary production (Chiswell et al., 2020; Thomsen et al., 2019; Thoral et al., 2022; Tait et al., 2021). For example, Tait et al (2021) report loss of giant kelp *Macrocystis pyrifera*, in response to the earlier marine heatwaves, although this impact may have been exacerbated by poor water clarity. Currently, New Zealand has no national marine environmental monitoring plan in place that would be able to detect changes resulting from MHWs (Ministry for the Environment, 2019) and there is limited long term temporal data for most coastal areas/ecosystems, although the Department of Conservation has just released its Marine Monitoring and Reporting Framework to guide how marine reserves in NZ are monitored in the future.

This study examines the most recent intense atmospheric heatwave (AHW) and associated MHW for the NZ region covering the austral warm season (November - March) for 2021/22, and compares this with the warm seasons of 1934/35, 2017/18 and 2018/19. It reports the atmospheric and oceanic drivers, describes impacts on selected marine and terrestrial ecosystems, including viticulture. Monthly to decadal atmospheric and oceanic mechanisms were investigated, along with an assessment of future likelihood of similar events.

[2] Argo is an international program of drifting buoys that collect information from inside the ocean using a fleet of robotic instruments that drift with the ocean currents and move up and down between the surface and a mid-water level. Each instrument (float) spends almost all its life below the surface.

2. METHODS

Many of the methods used here were described in Salinger et al (2019a) and Salinger et al (2021a). They are outlined briefly here, with new approaches described in more detail.

2.1 Observations of atmosphere and ocean temperature

The 22-station NZ air temperature (NZ22T) series (Salinger et al., 1992) was used to calculate monthly mean air temperature anomalies for 1934-2022, relative to the 1981-2010 normal. These were combined with SSTs for the NZ region of 4 million square kilometres (NZSST) to form combined NZ temperatures for the entire NZ area (NZEEZT) described by Salinger et al (2020). From the daily time series, extreme statistics TX90p (percentage of days when the daily maximum temperature is above the 90th percentile), TN90p (Percentage of days when the daily minimum temperature is above the 90th percentile), and number of days ≥25°C averaged over NZ during 1940-2022 were calculated as in Salinger et al (2019a) for NDJFM. Eight stations were analysed for the 1934/35 event. Monthly SST observations were obtained from Extended Reconstructed Sea Surface Temperature version 5 (ERSST; Huang et al., 2017).

Daily SST estimates came from the NOAA 0.25° daily Optimum Interpolation SST version 2.1 analysis (OISSTv2.1) (Huang et al., 2020) on a 0.25° latitude/longitude grid spanning September 1981-July 2022. These were area-averaged over the eastern Tasman Sea 160-172°E and 35-45°S as in Salinger et al (2019a). A subset of SST estimates from ERSSTv5 for 1934/35 and OISSTv2.1 for the remainder for NDJFMA was also extracted for all 0.25° grid cells that lay within the Exclusive Economic Zone (EEZ) of NZ, corresponding to an area 200 nautical miles in width seaward of the coastline.

The Hobday et al (2016; 2018) MHW definitions were applied to identify and characterise MHWs based on daily (i) area-averaged and (ii) EEZ grid cell SST estimates from OISSTv2.1 as in Salinger et al (2019a) using a MatLab implementation (Zhao and Marin, 2019) of the Hobday et al. (2016) MHW definition. Ocean sub-surface temperature from NOAA's Global Ocean Data Assimilation System (GODAS) data (Saha et al., 2006) were averaged between

40°S and 45°S, 140°E and 150°W, over the depth range 25 to 600m, and Argo profiles (Jayne et al., 2017) were extracted for the eastern Tasman Sea (160-172°E, 35-45°S).

2.2 Atmospheric circulation

For atmospheric circulation, monthly mean sea level pressures (MSLP) for NDJFM and 500hPa geopotential heights for NDJFM were obtained from the NCEP/NCAR Reanalysis (Kistler et al., 2001) and the ERA-Interim reanalysis (Dee et al., 2011). Several indices were used to characterize the circulation: Trenberth (1976) Z1 and M1 indices and weather regimes over NZ (Kidson, 2000) for the 2017/18, 2018/19 and 2021/22 heatwaves. Z1 measures west-east (zonal) flow and M1 south-north (meridional) flow in the NZ region: negative Z1 is typical in blocking situations when the prevailing westerly to southwesterly flow is absent in the region, especially with negative M1 (northerly flow anomaly). For large-scale circulation and monthly to decadal modes of variability the following were used: the Fogt et al (2009) Southern Annular Mode (SAM) reconstructed index, combined with the Marshall (2003) SAM index, the Southern Oscillation Index (SOI) of Troup (1965), and for the Interdecadal Pacific Oscillation (IPO) Tripole Index (Henley et al., 2015).

2.3 Ocean hindcasts

The ocean hindcast model is based on a global 0.25° configuration (Behrens et al., 2021; Madec et al., 2017; Storkey et al., 2018) and forced with JRA-55-DO v.1.5 (Tsujino et al., 2018) over the period 1958-2022. For this study the period 2000-2022 has been analysed and top 50m anomalies computed by subtracting the climatological mean over the period 2000-2022.

2.4 Recurrence interval of heatwaves

The extremes in a given year can be compared to the estimated distribution of temperatures for the period before that occurrence. A generalised extreme value distribution was fitted to the annual anomalies from the 66-year period 1871-1935, for the 1934/35 extreme, and the 66-year period 1957-2022 for the three more recent events. Expected probability of occurrence and the estimated recurrence interval (ERI) of the heatwaves were made based on the two distributions.

The probability of occurrence and recurrence intervals for a range of warming scenarios was estimated, with warmings of 1.5, 2, 3, and 4°C added to the early part of the record (the fifty years 1871-1920), which is considered close to the "preindustrial" temperature distribution. This was achieved by fitting generalised extreme value distributions to the observed temperature record for 1871-1920, plus the relevant warming offset. Such an approach was taken as it may capture the full distribution of temperature expected in future better than it would be by using climate model estimates.

2.5 Glaciers and seasonal snow

The end of summer snowline (EOSS) time series (Chinn et al., 2012) was used to estimate Southern Alps glacier mass balance from 1977 to 2021 for $EOSS_{Alps}$ (Salinger et al., 2019a). Regression relationships were employed to calculate $EOSS_{Alps}$ for 1935 and 2022, using Hermitage Mt Cook glacier season annual mean temperature, the SAM index, and Kidson (2000) Trough and Block regimes frequencies (Salinger et al., 2019b). The methods of Chinn et al (2012) were used to estimate downwasting and proglacial lake growth.

Estimates of water stored as seasonal snow in the South Island for 2021/22 were provided by the model "SnowSim", available through Meridian Energy Ltd (https://www.meridianenergy.co.nz/who-we-are/our-power-stations/snow-storage/; Garr and Fitzharris, 1996). SnowSim calculates water stored as seasonal snow for key hydro-generating river catchments and is tuned to their long-term water balance.

2.6 Agriculture

Grapes

Daily maximum and minimum temperatures (March 1947 to July 2022) were sourced from the regional meteorological station at the Marlborough Regional Station (41.48°S; 173.95°E). A temperature of 0°C was considered to be a damaging frost.

Grapevine phenology was estimated using a budburst model (García De CortázarAtauri et al., 2009) and estimated to occur when the accumulated growing degree days (base 5°C) and starting on July 1 (mid-winter in the Southern Hemisphere) had reached 294.4. The dates of flowering and véraison were estimated using the GFV model (Parker et al., 2013) and harvest defined as the date when fruit reaches a soluble solid concentration 20 °Brix (Parker, 2012).

Regional Marlborough yields and areas were sourced from annual New Zealand Winegrowers Vintage survey and Vineyard reports respectively and yield component data from New Zealand Winegrowers Vinefacts[3].

Summer Fruit

Harvest dates were gathered for three varieties of cherries and two varieties of apricots (Table 3) at the Plant and Food Research orchard in Clyde, Central Otago (45.20°S 169.32°E) for 2016-2022, where meteorological data were also obtained.

2.7 Marine ecosystems

Surveys in Northland and Fiordland were conducted in 2022. During the period of the MHWs in this region many sponges showed changes consistent with temperature stress (López-Legentil, 2008; McMurray et al., 2011; Hill et al., 2016; Marlow et al., 2018) and see Bell et al (2022) for full details of survey methods. These changes included the bleaching of sponges with photosynthetic symbionts and tissue necrosis. In Fiordland only *Cymbastela lamellata* was surveyed in Breaksea and Dusky sounds between 21 April and 3 June 2022 since this species was reported to have 'bleached'. Sponge bleaching results from the loss of symbionts from the sponge tissue, making the sponge turn from a dark brown to white colour. The proportion of healthy, partially bleached, and fully bleached sponges was estimated from photoquadrats surveys (10 x 1m^2 at each depth) by SCUBA Diving between 5, 10 and 25m.

Tissue necrosis of sponges was also reported from the north of New Zealand during the 2022 MHW period. The presence and severity of tissue necrosis affecting the massive sponges *Ecionemia alata* and *Stelletta conulosa* were made using existing photographic datasets, videos and in-situ observations at 1 - 20m depth throughout northeastern New Zealand (for full site locations see Bell et al. 2022). Data was collected between February and July 2022. The presence and condition of other sponge species were also noted but not quantified. *Ecionemia alata* and *Stelletta conulosa* were assessed as either healthy, partially sick (<20% visible necrosis) or sick (>20% visible necrosis) (Marlow et al., 2018) and see Bell et al (2022) for full details of survey methods.

Regular monitoring of kororā/Little Penguin (*Eudyptula minor*) nesting sites determined burrow occupancy, reproductive success (number of clutches laid and chicks fledged per pair), chick weights prior to fledging and chick body condition scores. These scores aimed to quantify the condition of the chicks by assessing pectoral muscle coverage over the keel; where a score of one is poor muscle coverage, two is moderate muscle coverage and three is good muscle coverage. Chick development was assessed by overall growth rate and feather development. Deceased kororā were either found washed ashore on Bay of Plenty coastlines (see Figure 13) and were deceased upon arrival or died shortly after and/or collected from Animal Rescue & Rehabilitation Centre Wildlife Trust (ARRC) and externally examined. Hotline calls received during spring/summer periods (September-February) from 2015-2022 were collated and assessed for trends related to SST, Mean Wind Speed, Mean Air Temperature and Total Rainfall. During 2021/2022 a total of 21 kororā were collected for mortality research from Bay of Plenty coastlines.

The diet of yellow-eyed penguins (*Megadyptes antipodes*) at Moeraki, North Otago, was investigated through eight years from 638 casts (vomited remains of indigestible hard parts of prey) and 126 spills (vomited remains of undigested or partially digested prey sometimes spilt during food transfers from adults to chicks) collected from June 2014 to May 2022.

3. RESULTS

3.1 Observations of atmosphere and oceans

3.1.1 Surface temperatures

The coupled ocean-atmosphere heatwaves in the NZ region during the four warm seasons (NDJFM) studied here were the most intense recorded in the NZ and Tasman Sea regions in 150 years of land-surface air temperature records, and ~40 years of satellite-derived SST records (Sutton 2019), as shown in Fig. 1a-f.

For all four heatwaves, both land air and sea temperatures combined were 1.1° to 1.4°C above the NDJFM 1981-2010 averages over the entire region (Salinger et al, 2020) (latitude 32° to 52°S, and longitude150°E to 180°) (Table 1 and Fig. 1.). NZ22T anomalies (Table 1) were 1.4°C, 1.7°C, 1.2°C and 1.2°C respectively (Fig. 1a and Table 1), by far the four warmest on record (Salinger 1979, Mullan et al.,

[3] https://www.nzwine.com/members/sustainability/vine-facts/20212022-season/

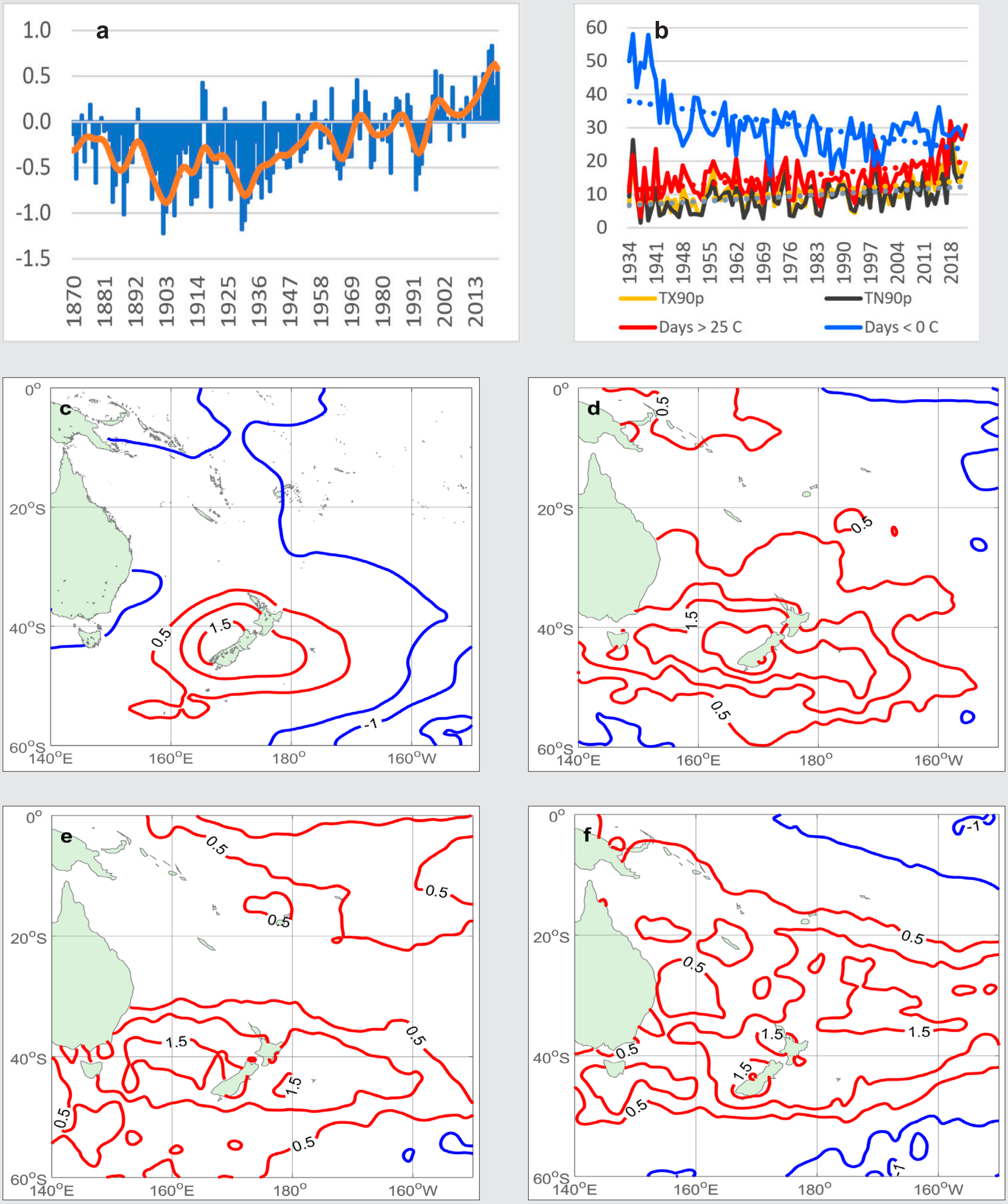

Figure 1: a. New Zealand 22 station air temperature anomalies (°C) (NZ22T) series (red smoothed) 1870-2022; **b.** Extremes – TX90p, TN90p and days >25°C and <0°C averaged over New Zealand 1934-2022; **c.** ERSSTv5 1934/35; **d.** OISSTv2 2017/18; **e.** OISSTv2 2018/19; and **f.** OISSTv2 2021/22. For panel c the climatology period is 1981-2010; and for panels d-f, the climatology period is 1982-2011 and all for the period of NDJFM.

2010). Indices of temperature extremes for NZ (Table 1 and Fig. 1b) show that the percentages of annual warm days above the 90th percentile were 26%, 33%, 22% and 19% respectively. Counts of summer days ≥25°C averaged 22, 32, 26 and 31 days nationwide for the four warm seasons respectively. All these values were statistically significant (Table 1).

For the Tasman Sea and east of NZ (32°–52°S, 150°–

METRIC	1934/35	2017/18	2018/19	2021/22
NZ22T	**+1.37**	**+1.72**	**+1.17**	**+1.19**
ERSSTv5	**+1.07**	**+1.37**	**+1.10**	**+1.10**
NZEEZ	**+1.09**	**+1.39**	**+1.10**	**+1.01**
SAM	**+1.37**	**+1.33**	**+1.66**	**+2.16**
NINO3.4	+0.10	-0.90	+0.79	-0.97
SOI	**+5.0**	**+4.8**	-2.2	**+10.5**
IPO	-0.021	**-0.925**	-0.146	**-1.328**
Z1	**-23**	**-17**	-11	**-33**
M1	**-52**	**-27**	**-35**	-3
Trough	NA	-6.7	**+7.7**	**-10.7**
Zonal	NA	-15.5	**-3.8**	**-15.1**
Block	NA	+22.6	**+6.4**	**+26.0**
Warm days TX90p	**26**	**33**	**22**	**19**
Warm nights TN90p	**26**	**29**	**17**	**16**
Days ≥25°C	**22**	**32**	**26**	**31**

Table 1: Indices for the four heatwaves for NDJFM. NZ22T is the 22 station NZT series for surface temperature over the land area of New Zealand, ERSST is the ERSST version 5 for the New Zealand (NZ) Exclusive Economic Zone, 34 to 48°S, and 165° to 179°E, and NZEEZT are NZ22T and ERSST combined and weighted for the entire NZ region with anomalies in °C. All temperature departures are anomalies from the 1981-2010 climatology period for the months of November – March. NZ22T mean 0.02°C, standard deviation (s.d.) of ±0.42°C, ERSST mean 0.0, s.d ±0.29°C, and NZEEZT mean -0.2 s.d ±0.54 °C. SAM the Southern Annular Mode (Fogt et al 2009) mean 0.06, s.d 1.08, Nino3.4 the Index mean 0.0, s.d 1.3, the Troup Southern Oscillation Index (SOI, Troup 1965) mean 0.0, s.d. 1.0 and the Interdecadal Pacific Oscillation (IPO) the tripolar index (Henley et al., 2015) mean -0.9, s.d. 0.83. Z1 (mean +0.3 s.d. 14.5) and M1 (mean +1.2, s.d, 19.6) are Trenberth (1976) zonal and meridional indices. Kidson regimes are Trough, Zonal and Block anomalies (Kidson 2000). TX90p and TN90p are the percentages of days above the maximum (TX) and minimum (TN) daily 90 percentile (mean is 10% 1981-2010 climatology period, with Days ≥25°C counts, all averaged for 26 NZ climate stations. Mean counts days ≥25°C 15.0, d ±5.2 days. Bolded values significant at p<0.05.

180°E) the four periods were characterised by SSTs 1.1°C, 1.4°C, 1.3°C and 1.2°C above average (Figs. 1c-f), the largest anomalies on record. The three earlier periods also showed a similar spatial pattern with highest anomalies to the west of the South Island of NZ, whilst the last was broader in extent.

Applying a MHW definition (Hobday et al., 2016) to daily area-averaged SST from OISSTv2.1 for the eastern Tasman Sea (Fig. 2) showed that the region experienced MHW conditions for 292 days (d) August 2021 to July 2022 (Fig. 2a-b), the highest annual number of MHW days observed for this area over all corresponding annual periods during the satellite-era (1981-present). The majority (79%) of these days during the 2021/22 period were ranked as a Category I (Moderate) event from an areal average (Hobday et al., 2018), with the remainder (21%) as a Category II (Strong) event. The longest continuous MHW occurred during austral autumn and lasted 158 days (Feb 24 2022 – Jul 31 2022) peaking as a Category II (Strong) MHW with a mean intensity of 1.3°C (Fig. 2a,c). This is the second longest individual MHW detected in the eastern Tasman Sea, having a similar duration but reduced intensity and later onset and decay period compared to the summer 2017/18 and 2018/19 events. In comparison, the 2017/18 MHW lasted for 153 days, peaking as a Category IV (Extreme) MHW, with a maximum (mean) intensity of 3.8°C (2.0°C), whilst the 2018/19 MHW lasted for 173 days, peaking as a category II (Strong) MHW with a maximum (mean) intensity of 2.7°C (1.6°C).

Applying a MHW definition to daily SST from OISSTv2.1

grid cells within the New Zealand EEZ (200 nautical miles in width seaward of the coast; Fig. 2d-g) reveals marked spatial variation in the duration and severity of MHWs in coastal waters between August 2021 and July 2022. The most prolonged MHW conditions were experienced along the western coast of the North Island and southeast coast of the South Island (>200 days), with the majority (>70%) of these days ranked as a Category I (moderate) conditions (Fig. 2d). Category II (strong) conditions were largely restricted to the western coast of the North and South Islands, where they were established for a total of 40-60 days depending on location (Fig. 2e). Similarly, Category III (severe) and IV (extreme) conditions were also mostly limited to the northwest and southwest coastlines of New Zealand and were present for a total of 10 - 20 days (Fig. 2f-g). MHW conditions were generally most short lived (50-100 days; Fig. 2d-e) adjacent to the southeast coastlines of the North Island (e.g. east of 176°E) and within the Subantarctic Zone (e.g. south of latitude 48°S).

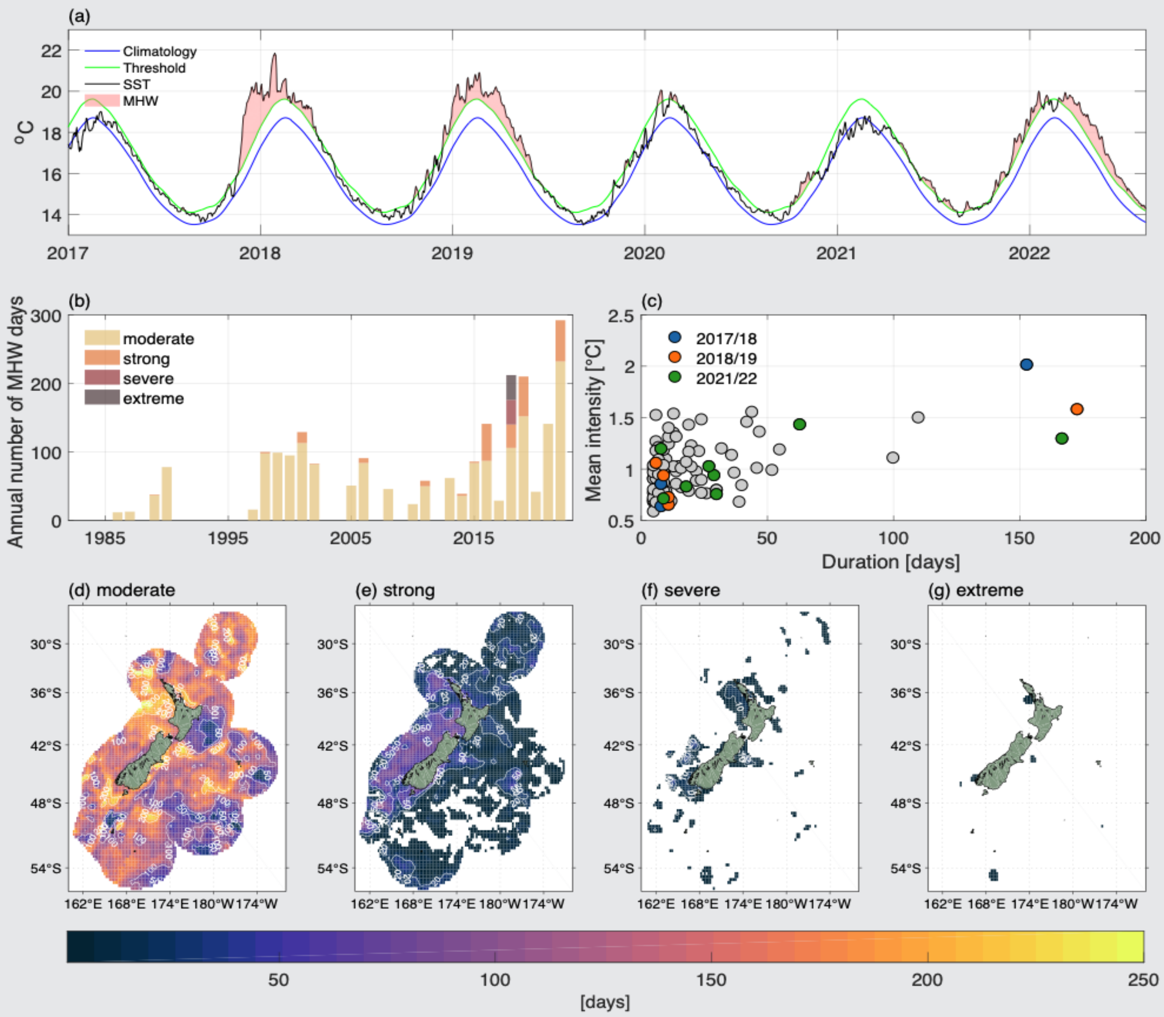

Figure 2: a. Time series of area-averaged sea surface temperature (SST) climatology (1981-2011; blue), 90th percentile MHW threshold (green) and January 2017 to July 2022 SSTs (black) for the eastern Tasman Sea (160-172°E, 35-45°S). The red shaded regions identify periods associated with MHWs using the Hobday et al. (2016) definition. **b.** Annual number of days that the eastern Tasman Sea was in a MHW. The shaded regions identify the number of days spent in one of the four MHW categories based on the Hobday et al. (2018) MHW categorization scheme. The summation in (b) has been performed over 12 month periods of August to July in consecutive years. **c.** The duration and mean intensity of each MHW detected in the area-averaged SST time series for the eastern Tasman Sea. Individual MHWs detected in the 12-month periods of August to July of 2017/18, 2018/19 and 2021/22 are shaded. **d-g.** The number of days each 0.25° lat-lon OISSTv2.1 grid cell within the New Zealand EEZ spent in one of the four MHW categories based on the Hobday et al. (2018) MHW categorization scheme between August 2021 and July 2022.

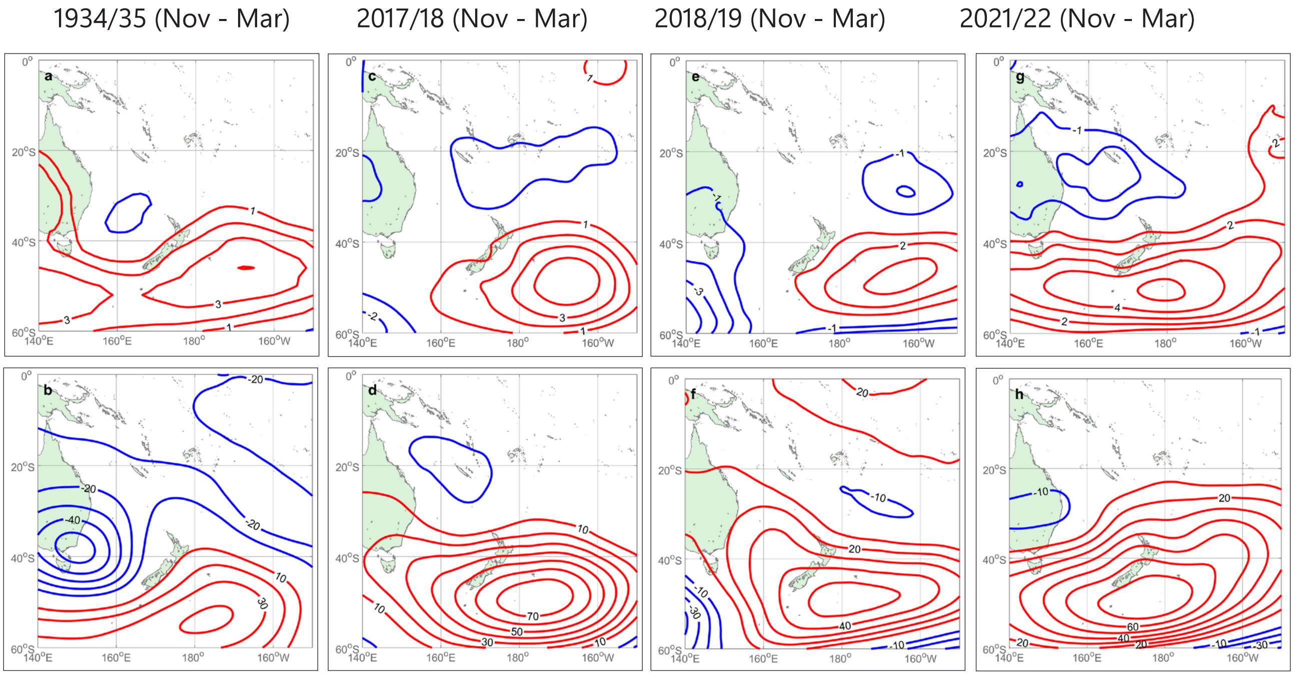

Figure 3: Atmospheric circulation patterns. NDJFM mean sea level pressure anomalies (1981-2010 climatology): **a.** 1934/35, **c.** 2017/18, **e.** 2018/19 and **g.** 2022. NDJFM 500hPa Geopotential Height anomalies (1981-2010 climatology): **b.** 1934/35 **d.** 2017/18, **f.** 2018/19 and **h.** 2021/22. Please note that 1934/35 data are based on the 20th Century Reanalysis dataset (Compo et al., 2011); for the other time periods, the NCEP-DOE AMIP-II Reanalysis dataset was employed (Kanamitsu et al., 2002).

3.1.2 Atmospheric circulation

The four NDJFM seasons (Fig. 3a, 3c, 3e and 3g) show a pattern of blocking (persistent higher than normal pressures): in 1934/35 to the south and southeast of NZ, with negative pressure anomalies northwest of NZ, and the other three very strong blocking to the southeast of NZ and negative pressure anomalies to the north. The M1 and Z1 circulation indices showed northeasterly airflow for 1934/35, 2017/18 and 2018/19. Airflow was easterly for 2021/22. Kidson weather regimes showed a lack of zonal regime for the recent three warm seasons (NDJFM) and more blocking throughout the season especially for 2021/22, where troughing was also absent.

The 500-hPa geopotential height anomalies were extremely consistent (Fig. 3b, 3d, 3f and 3h) with very strong blocking to the southeast of NZ, with average positive height anomalies of 50 geopotential metres or more in the most recent three. The 1934/35 had positive height anomalies extending west of the North Island over the north Tasman Sea. The 2017/18 and 2021/22 anomalies were the most intense, reaching 70 geopotential metres (gpm) to the southeast of the South Island.

Over the austral warm season 1934/35 and 2021/22 the SAM was very positive, although no records were set (Table 1). The SAM was also positive during 2017/18 and 2018/19. The Oceanic Niño Index (ONI) showed weak activity in 1934/35 (Niño 3.4 +0.1) but stronger in 2018/19 (+0.8). The 2017/18 and 2021/22 were in the La Niña phase (+0.9 and +1.0 respectively) for the ONI moderately so, and the IPO strongly negative with very high Southern Oscillation Index (SOI) values (Table 1).

3.1.3 Ocean Sub-Surface Temperature

GODAS sub-surface ocean temperature patterns for (November - April) NDJFMA 2017/18, 2018/19 and 2021/22 for the latitudes 40-45°S (Fig. 4a-c) indicate very shallow positive anomalies west of the South Island, with a narrow band down to about 50m east of the South Island.

Positive SST anomalies also existed in the western Tasman Sea and into the South Pacific east of NZ. The Argo measurements (Fig. 4d) averaged over the eastern Tasman Sea confirmed surface warming from November to February, peaking at 3°C mean anomaly in 2017/18 and 1.5°C in 2018/19, both with shallow anomalies to the upper 20m. A different signal occurred for 2021/22, much weaker, but much more persistent from October to April, and extending all the way down to 150m in 2022.

3.1.4 Ocean hindcasts

The top 50m November - March modelled temperature anomalies for 2018/19 and 2019/20 are spatially very coherent (Figs. 5a-b). Positive temperature anomalies in the order of 1°C were found over the Tasman Sea and anomalies near the Chatham Rise in both years reached 1.5°C for this five-month period. The anomaly pattern for 2021/2022 differed in the shape (Fig. 5c) compared to the other two periods. The western part of the Tasman Sea, near Australia, did not exhibit positive temperature anomalies over this depth range, while the positive temperate anomalies extended further north and east of New Zealand compared to the other two periods. Conversely, anomalies over the Campbell Plateau and southeast of the Chatham Rise were lower in 2021/22. The difference in the top 50m temperature anomaly pattern between these three periods matches the atmospheric anomalies (500hPa Figs. 3-d, f, and h) and associated wind anomalies. Area averaged top 50m temperature anomalies around New Zealand (Fig. 5d) reveal how different these three periods were compared to previous years. November-March 2017/18 showed the largest peak anomalies for this region and reaching 0.9°C in February. Nevertheless, positive temperature anomalies for 2018/19 and 2021/22 for these two periods persisted into early winter (June), which has not been observed previously. However, climate projections with New Zealand's Earth System Model suggest that this might become the new normal, where positive anomalies disproportional extend into autumn as the ocean warms under climate change (Behrens et al., 2022).

3.1.5 Recurrence interval of heatwaves

Based on the temperature distribution up to 1934/35 (Fig. 6a) the 1934/35 summer was very rare with a

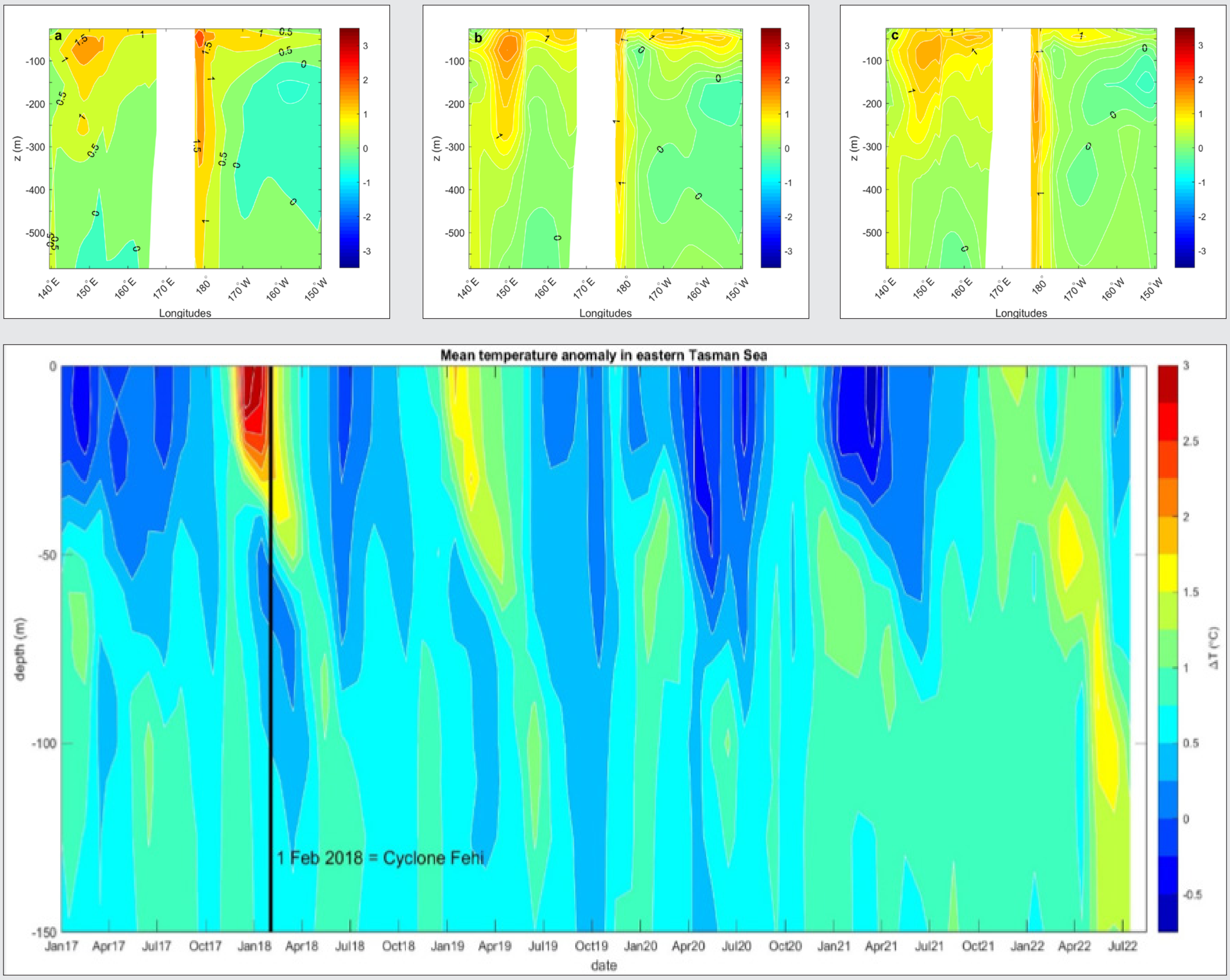

Figure 4: Subsurface temperature anomalies. **a, b, c** and **d.** GODAS subsurface Tasman Sea, 40°S and 45°S, 140°E and 150°W, over the depth range 25 to 600m. **a.** NDJFM 2017/18 **b.** NDJFM 2018/19 and **c.** NDJFM 2021/22 and **d**. Eastern Tasman Sea from Argo floats January 2017 – 4 April 2022.

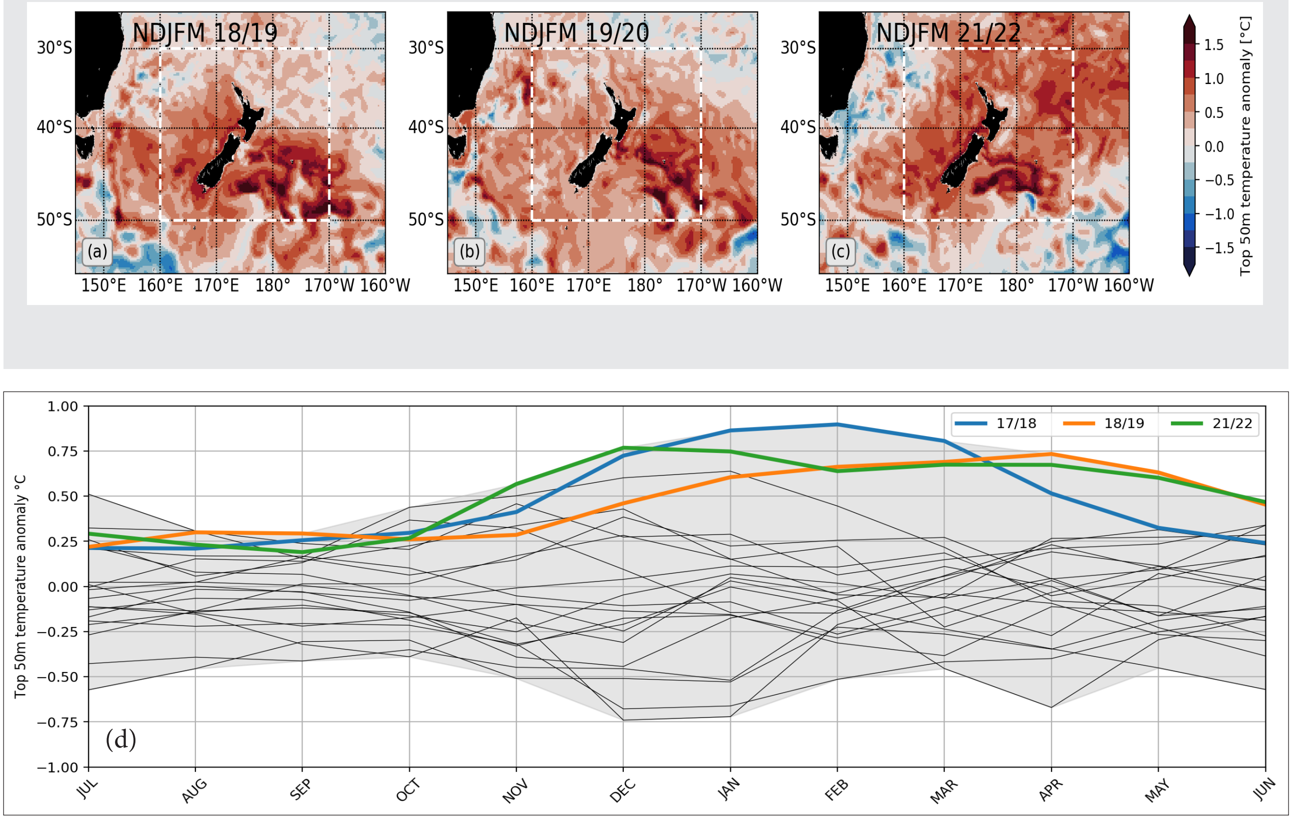

Figure 5: Modelled top 50m temperature anomalies relative to the climatological mean over the period 2000-2022. **(a)** November-March 2018/19, **(b)** November - March 2019-2020 and November - March 2021/22. **(d)** Top 50m area-averaged temperature anomalies over the region 160°E-170°W and 50°S-30°S (white dashed box in a-c) for individual years from 2000-2022 (black lines). The three warmest summers (a-c) are colour coded.

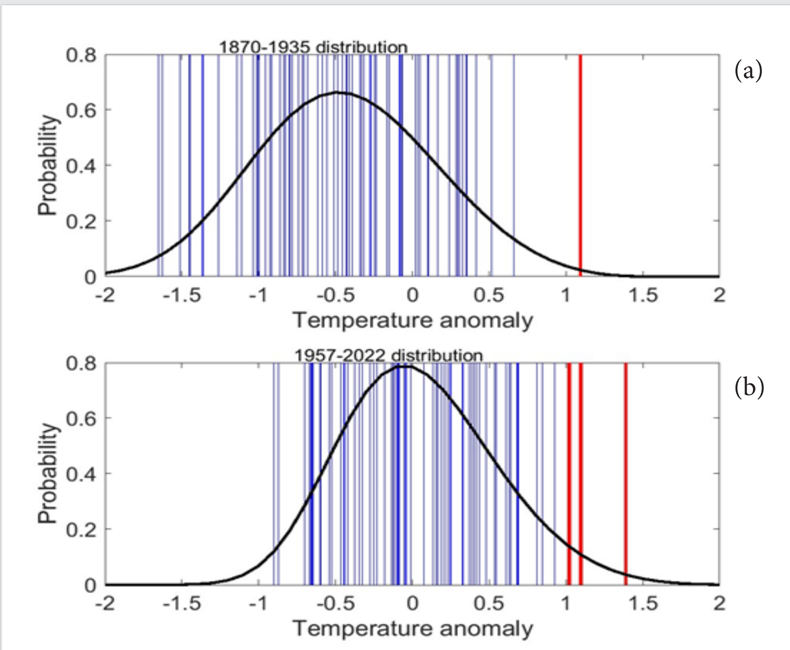

Figure 6: Probability of extreme warm season periods (November – March) for the period before that occurrence. (a) 1870 – 1935, and (b) 1857 – 2022. Heatwave seasons marked in red (see Table 1) and all other seasons in blue. The black lines show fitted GEV distributions.

probability of occurrence of 0.003, or an ERI of around 320 years. Using the 1957-2022 distribution, the 1934/35 event is still relatively uncommon, with an estimated ERI of around 40 years (Fig. 6b). For the recent extreme warm summers, compared to the temperature distribution from 1957 to 2022 (Fig. 6b), we find the two most recent have ERIs of around 30 years while 2017/18 has an ERI of around 150 years.

In the estimated future distributions with 1.5° or 2°C warming (added to the 1870-1920 distribution), such a summer would be common even under 1.5°C warming with ERIs of 2-3 years. Under 2°C warming, those years would all be cooler than average and would be occurring, as cool years, approximately one to two times per decade. Under the current climate warming trajectory this would be reached around the 2060s (Mullan et al 2016).

It is notable that with three or more degrees of warming (from the 1871-1920 period), all four of the heatwaves discussed here would count as unusually cold summers, with ERIs (for cold summers) of 40 years or more for 3 degrees of warming, and in the thousands of years for 4 degrees of warming.

3.2 Glaciers and seasonal snow

3.2.1 Glaciers

Ice volume loss in the Southern Alps for the small and medium glaciers was estimated to be 0.4km^3 volume in 1934/35, 2.1km^3 in 2017/18, 2.0km^3 in 2018/19 and 1.7km^3 for 2021/22.This totals 5.9km^3 for the three recent heatwave warm seasons, 22% of the total ice volume of the Southern Alps in the 1977 inventory (Chinn 2001). For the three recent heatwave summers, total losses from all glaciers amounted to 9.3km^3, 17% of the 1977 total (Fig. 7a). The 2018 – 2022 period represents the largest ice loss in any 5-year period since 1949 (Salinger, et al 2021).

3.2.2 Seasonal snow

The 1934-1935 snow year was likely remarkable. Water stored as seasonal snow reached a maximum that was just below average at 402mm water equivalents (w.e.) in mid-October, based on SnowSim model estimates. Rapid snowmelt began in mid-November and all snow had disappeared by 11 January, the third earliest date for the 1930-2019 period (Fitzharris and Garr, 1995; de Latour, 1999). Melt rate over this period was 6.5mm/d w.e., the highest of the four summers. The earliest date for disappearance of all seasonal snow is 28 December for the 1974-75 snow year, but this was from a maximum of only 198mm w.e., amongst the lowest since 1930.

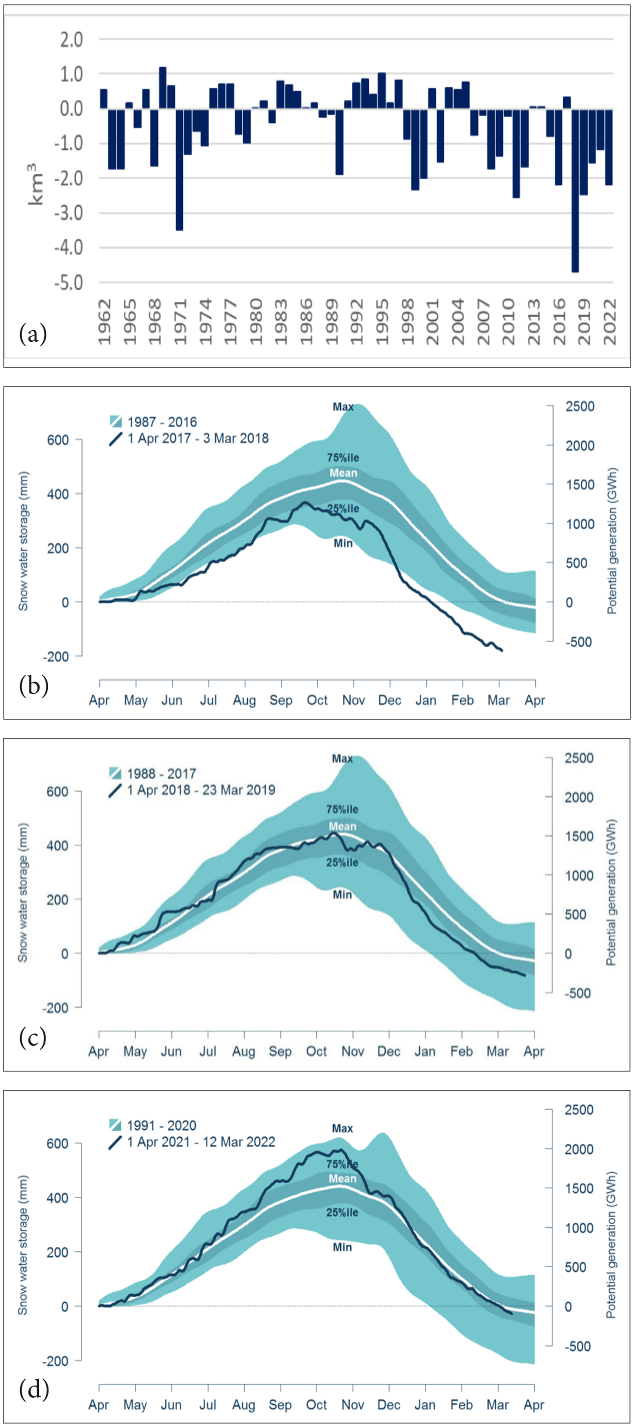

Figure 7: Southern Alps ice volume and seasonal snow. **a.** Southern Alps ice volume change (km^3 of water equivalent), between years, for all glaciers of the Southern Alps from 1962 to 2022. **b-d**. Estimated water stored as seasonal snow (mm) from SnowSim for the period 2017 – 2022.

During the 2017-18 snow year, the estimated water stored as seasonal snow leading up to August (Fig. 7b) was very low. It reached a maximum of 30% of average at 350 mm w.e. in late September, much earlier than usual. Rapid melt began on 18 November and from mid-December 2018 the snowpack was the lowest on record. By 10 January all the seasonal snow had melted, the second earliest date since 1930, with extraordinary loss of permanent glacier snow and ice. Melt rate over this period was 5.7mm/d w.e. SnowSim estimated that maximum accumulation for the 2018-19 snow year was close to average at 420mm w.e. and occurred in late October (Fig. 7c), slightly later than normal. There was rapid melt from late November, but it took until 12 February for all the seasonal snow to disappear. Melt rate over this period was 5.0mm/d w.e.

For the 2021-22 snow year, the estimated water stored as seasonal snow leading up to the peak (Fig. 7d) was very high. It reached a maximum of 135% of the normal. There was rapid melt from late November, but it took until 12 February for all the seasonal snow to disappear. Melt rate over this period was 5.0mm/d w.e. 410mm w.e. in late October, at the usual time. Rapid melt began at the beginning of November and by 1 March 2022 the snowpack was totally depleted, and reached the 25 percentile by the end of March, representing the loss of 50mm. By early March all the seasonal snow had melted, with a loss of permanent glacier snow and ice. Melt rate over this period was 1.7mm/d w.e.

3.3 Agriculture

Grapes

The mean daily temperature during the flowering, the period defining fruitset and berry number per bunch periods of 2021 and 2022 was 16.8 and 18.9°C respectively. The seasonal differences were largely the result of a cold six-day period in the middle of flowering in the 2021 vintage where daily temperatures did not exceed 15°C.

Seasonal differences in grapevine yield ranged from a high of 15.2 and 7.56 Tonnes/hectare (T/ha) for the 2022 Sauvignon blanc and 2020 Pinot noir harvests respectively, to a low of 10.3 and 3.59T/ha in 2021 (Fig. 8), likely reflecting these seasonal differences driving bunch mass differences (Table 2). However, for Sauvignon blanc, bunch mass differences largely reflect differences in berry number per bunch rather than berry mass, but the reverse was true in Pinot noir, where berry number per bunch were more similar and berry mass varied, particularly between 2021 and 2022 (Table 2). The difference between the varieties is

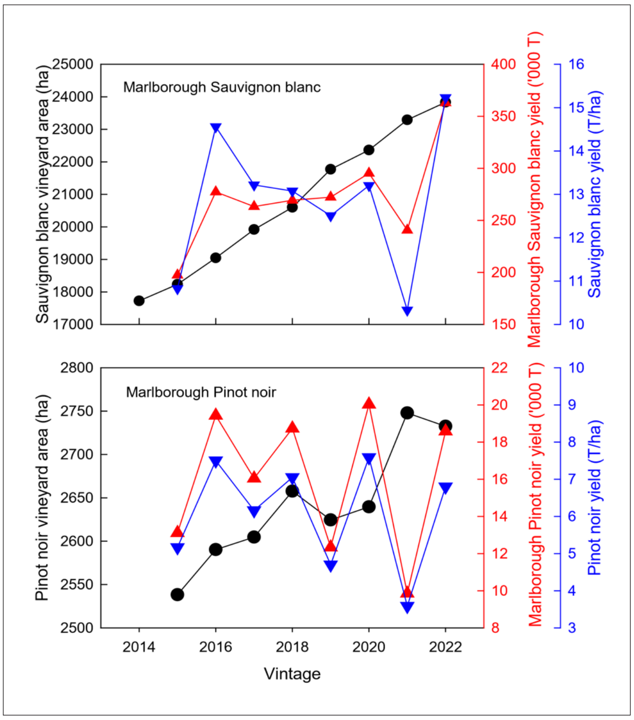

Figure 8: Seasonal variation in Marlborough Sauvignon blanc and Pinot noir vineyard areas and grapevine yields. ● Vineyard area, ▲ Marlborough grape yield, ▼ Marlborough grape yield per ha.

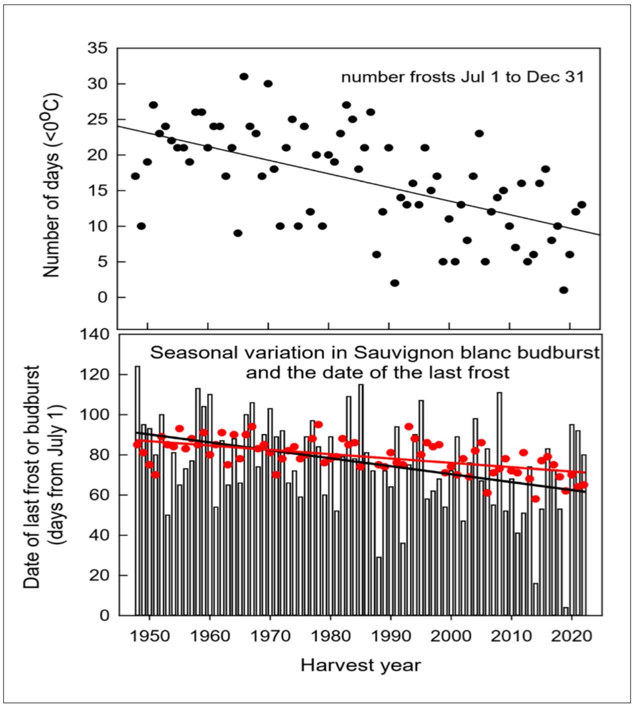

Figure 9: Number of Marlborough spring frosts (<0°C) (1 July to 31 December) (upper) and the date of the last frost and estimated date of Sauvignon blanc budburst (lower).

Bars = date of last frost and ● = date of budburst.
Date (days from July 1) of last frost =861-0.40x; date of budburst = 507-0.216x.

	AVERAGE		VINTAGE				
		Cv*	2018	2019	2020	2021	2022
PINOT NOIR	**2015 - 2022**	**2015 - 2022**					
Average bunch mass (g)	68.0	29.0	109.7	48.4	70.9	43.4	68.14
Average berry mass (g)	1.2	18.9	1.62	0.90	1.11	0.92	1.26
Average berry number per bunch	58.2	11.7	67.9	53.8	63.7	47.2	54.1
Inflorescence number per m row	24.4	14.4	23.7	32.0	21.2	27.3	20.2
SAUVIGNON BLANC	**2017 - 2022**	**2017 - 2022**					
Average bunch mass (g)	128.5	18.5	156.6	126.7	144.7	90.3	145.1
Average berry mass (g)	2.0	10.3	2.2	1.7	1.8	1.8	2.1
Average berry number per bunch	64.1	16.3	73.2	73.7	78.4	49.3	69.1
Inflorescence number per m row	23	12.9	24	23	20	26	25
	1948 - 2021	**1948 - 2021**					
Initiation temperature (°C)	17.4	6.1	17.9	18.7	19.2	15.9	17.4
Flowering temperature (°C)	17.1	6.3	18.8	19.1	16.4	16.9	19.0

Table 2: Sauvignon blanc and Pinot noir yield components.
*cv = coefficient of variation

		2016	2017	2018	2019	2020	2021	2022
Cherry	'Lapins'	12/1	18/1	31/12	9/1	10/1	4/1	5/1
	'Sweetheart'	25/1	18/1	8/1	12/1	15/1	5/1	10/1
	Staccato®	29/1	3/2	15/1	22/1	25/1	21/1	12/1
Apricot	'Nzsummer2'	3/2	6/2	19/1	30/1	31/1	26/1	31/1
	'Nzsummer3'	9/2	20/2	26/1	9/2	7/2	9/2	1/2

Table 3: Harvest dates of summerfruit in Central Otago.

largely a reflection of the ability of Pinot noir to set seedless berries (resulting in millerandage - a potential viticultural hazard problem in which grape bunches contain berries that differ greatly in size and, most importantly, maturity), whereas few seedless berries are observed in Sauvignon blanc.

The number of days with minimum temperatures between 1 July and 31 December less than 0°C has consistently reduced between 1948 and 2022 (Fig. 9) and the date of the last frost has advanced by 0.40 days per year over the same period (Fig. 9). However, warming of mean daily temperature 0.019°C /day between 1 July and 31 August (Fig. 9) has also advanced the date of budburst

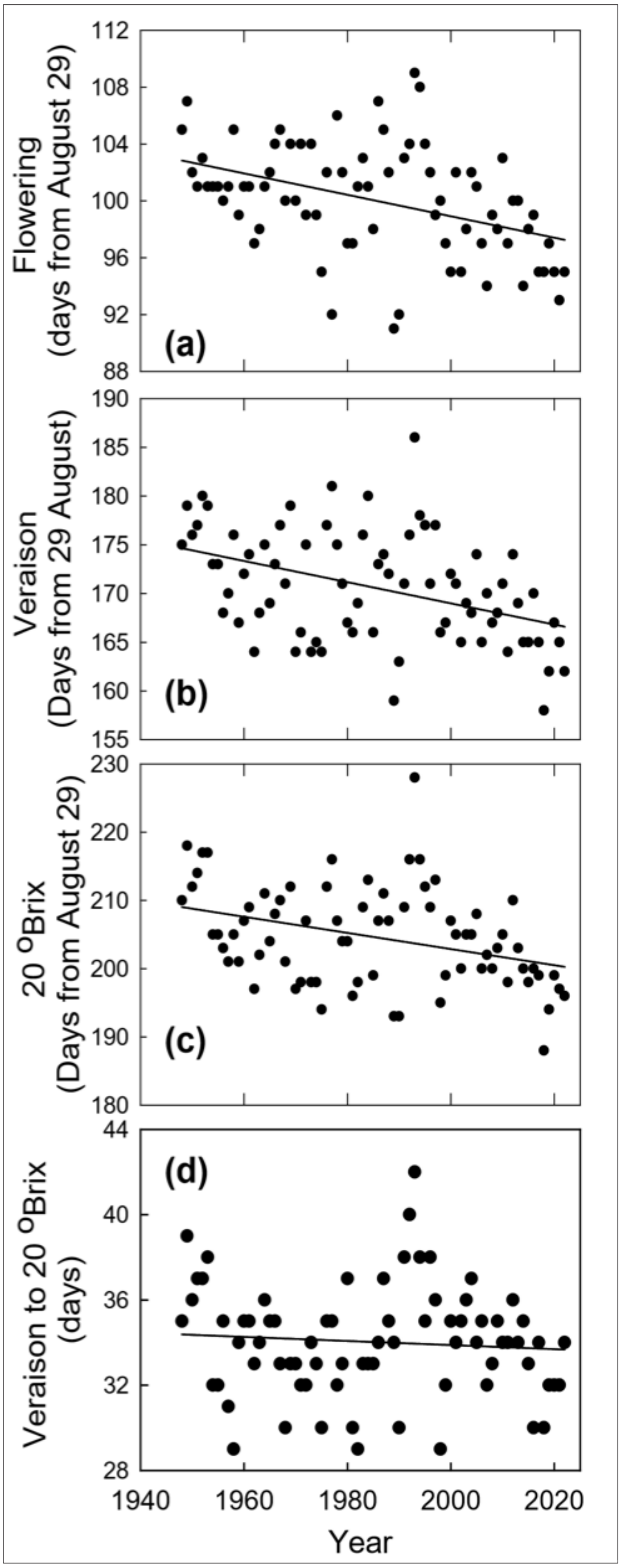

Figure 10: Seasonal changes in grapevine phenology estimated using GFV model (Parker et al., 2013) (Parker, 2012).

by 0.26 days per year, with the result seasonal frost risk has changed little over the past 74 years.

The GFV model simulations of flowering, véraison, and harvest dates advanced since 1948 (Fig. 10) and reflect an average increase in temperature of 0.013°C / day in the spring period (1 September to 30 November). Similar, but smaller temperature increases occur between 1 December and 15 February (0.011°C /day) but this advance had little effect on the average temperature over the flowering period, which has increased on average by 0.01°C per year. Similarly, there was little increase during ripening between 16 February and 15 April (0.001°C /day).

Summer Fruit

Of the AHW season's data available, September to January temperature departures from normal for 2018, 2019 and 2022 were +2.2, +0.6 and +1.0°C. For the three cherry varieties, 2018, 2019 and 2022 harvest dates averaged 13, 8 and 13 days respectively ahead of 2016 (a normal season). For apricots, the three AHW summers were 15, 3 and 6 days ahead of normal.

3.4 Marine ecosystems and impacts

In northeastern New Zealand, sponge necrosis was recorded at depths between 1–20m across including *Ecionemia alata* and *Stelleta conulosa*, with other unquantified reports of tissue loss/regression of *Stelletta maori*, *Cliona celata*, *Dendrilla rosea*, T*ethya* spp. and detached *Polymastia* spp. being washed up on the shore. Up to 45% of sponges observed in this region showed signs of necrosis. The greatest impacts appeared to occur on *Ecionemia alata* and *Stelleta conulosa*, where many sponges detached or had the appearance of "melting" off the reef. These species are two of the most common and important habitat-forming species across New Zealand's subtidal rocky ecosystems (although not found as far south as Fiordland). The densities of these two species are conservatively around 1 per 10m^2 (noting a single sponge can occupy up to 1m^2 of reef), with a distribution extends from approximately 5 to >100m depth. Given that necrotic sponges were reported at sites across > 500km of coastline, down to 20m, conservatively hundreds of thousands of sponges are likely to have been impacted (see Bell et al. in press for further information).

In May 2022, correlating with the maximum intensity of the MHW impacting the Fiordland region, widespread sponge 'bleaching' of *Cymbastella lamellata* was reported. Subsequently necrotic and dying sponges across several species were reported in northeastern New Zealand. Greater

Figure 11: Detached and rotting Anchorinidae sponge, Northland, April 2022.

than 90% of *Cymbastella lamellata* observed showing signs of either partial or complete bleaching in Dusky and Breaksea Sounds (Figure 11); There was no difference in the level of bleaching between depth and Remotely Operated Vehicle observations found bleached sponges to 50-60m (max depth sponges were found). While *C. lamellata* was the only species that appeared to be impacted in Fiordland, its high abundance across the region (average 1-10 per m^2 and a coastline of >600km) and depth distribution ranging from 5–60m, indicates that tens of millions of sponges could have been bleached. Some sponges, like *C. lamellata*, contain photosynthetic symbionts, and under temperature stress can expel these symbionts (López-Legentil, 2008).

Large marine impacts may be linked to starvation of kororā in the Bay of Plenty, with reduced chick body mass and condition in 2020 and 2021 compared to 2019, emaciated deceased chicks found in burrows and the highest volume of rescue calls received in 2021, since 2015 (McLuskie, 2023). Regular monitoring of kororā nest sites determined burrow occupancy, reproductive success (number of clutches laid and chicks fledged per pair), chick weights prior to fledging and chick body condition scores (McLuskie, 2023). Mean body mass and body condition of six-week-old kororā chicks in Mount Maunganui (Bay of Plenty) decreased by 19% during the 2020 and 2021 breeding seasons compared to 2019, which coincided with La Niña conditions and increased SST (Table 4). Chick development in 2020 and 2021 was slower than observed in 2019, with a delay in feather development and overall body size of chicks appeared smaller. Chick productivity was slightly lower in 2021 (1.22 chicks per pair), compared to previous seasons (Table 4). Six deceased emaciated chicks were also found within breeding burrows in the 2021 season, that most likely died of starvation. The proportion of burrows occupied by non-breeding birds during the day increased from 5% (2/38) in 2019 to 24% (15/63) in 2021 (Table 4).

The number of kororā rescue calls received by Western Bay Wildlife Trust (WBWT) for the Bay of Plenty region, increased significantly during the 2021/2022 Spring/Summer period (Sep-Feb) when mean Northern North Island SST were warmest (Fig. 12)(McLuskie, in press). Higher than usual call volumes in 2020/2021 and 2017/2018 were also consistent with increased SST. Rescuers observed and received multiple reports of deceased kororā washed ashore across the entire Western Bay of Plenty coastline (see Figure 13) over the 2017/2018 summer period (Graham, pers. comm). Increased call volumes in 2016 were inconsistent with SST trends, however had the highest mean wind speed (4.5m/s) between 2015-2021 spring/summer seasons. In spring/summer of 2021, 13 kororā rescues were attended and 77% (10/13) were found in a weak/exhausted state. Over half of deceased kororā specimens (57%) collected between 2021-2022 spring/summer (n=21) were found in an emaciated condition upon external examination and suspected to have died of starvation, however further research is needed to confirm cause of death.

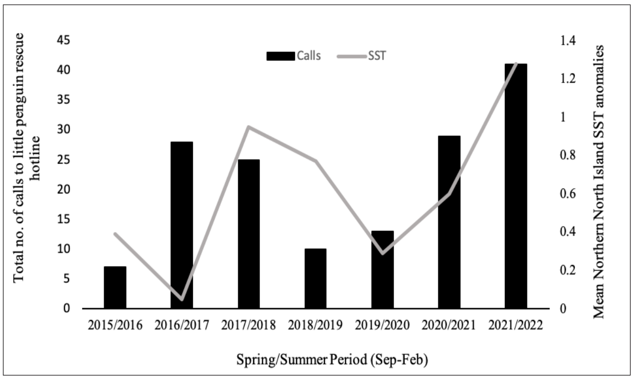

Figure 12: Calls to Western Bay Wildlife Trust kororā rescue hotline. Bay of Plenty, NZ, for 2015-2022 spring/summers (Sep-Feb).

Pilchard *Sardinops sagax* and anchovy *Engraulis australis*, two species of small pelagic nearshore fishes common around most of New Zealand, are absent from Otago, southeast South Island (Roberts et al. 2015, McMillan et al, 2019), where the relatively cool waters of the Southland current flow northward over the continental shelf (Sutton 2003, Stevens et al. 2021). A recent exception to this absence was a mass stranding of pilchard near Oamaru, North Otago in December 2019 (MacLean 2019). Through the eight years of sampling yellow-eyed penguin

Breeding Season (Jul-Feb) * La Niña	**Ocean Conditions**		**Productivity**			**Chick Health**			**Burrow Occupancy**	
Year	SOI-RM Rolling 3 month average	Mean SST (Nthn North Island)	n	Chicks per pair	Replacement clutches (Second clutch following first clutch failure)	n	Mean Mass (g)	Body Condition Score (1-3)	n	Non-breeding bird occupancy rate %
2019	-0.41	0.34	20	1.30	7	10	951	2.4	38	5
*2020	0.76	0.59	32	1.31	4	14	768	1.93	51	8
*2021	0.94	1.13	36	1.22	1	19	768	1.95	63	24

Table 4: Burrow occupancy, chick production and health in kororā based in Mount Maunganui, North Island, NZ, and associated ocean conditions (Southern Oscillation Index and Sea Surface Temperature) 2019-2021 (McLuskie, 2023).

prey remains at Moeraki from June 2014 to May 2022, pilchard and anchovy were each recorded only once. In both cases they were recorded in the most recent year, with two pilchard in a cast on 27 July 2021 and one anchovy in a spill on 14 August 2021. Both records coincided with a marine heat wave and may signal a future change in diet of yellow-eyed penguins with warmer ocean temperatures at Moeraki. If this is the case, then there would be an expectation of future increasing occurrences of pilchard and anchovy in the ongoing study of diet of yellow-eyed penguins at Moeraki.

4. DISCUSSION AND CONCLUSIONS

Heatwaves are becoming a major impact of global warming with the Intergovernmental Panel on Climate Change 6th Assessment Report (Seneviratne et al., 2021) indicating likely increases in unusually warm days and nights across most continents, and several occurrences of MHWs in 2020 (Blunden and Boyer, 2020). The unprecedented heatwave in the 2017/18 austral summer, coupled with a combined AHW/MHW event (Salinger et al., 2019a) was one example.

Although Perkins-Kirkpatrick et al (2018) suggests that the 2017/18 MHW would have been "virtually impossible" without an anthropogenic influence, the 1934/35 event indicates a similar episode has occurred in the past which was only 0.3°C cooler, without any allowance for anthropogenic global warming. Hence, it is important to examine similar AHW/MHWs in the NZ region in the climate record to document drivers and impacts. Srinivasan et al (2021) found that in the last decade monthly temperature extremes are increasing 4-5 times faster than expected in a climate with long term warming, and that the increase in extremes is faster than the rate of increase in mean temperature.

Four such austral warm season events occurred – in decreasing order of magnitude 2017/18, 1934/35, 2021/22 and 2018/19. The heatwaves had very similar atmospheric and oceanic footprints, covering all the land area, the entire central and south Tasman Sea and across to 180°E in the southwest Pacific. The recent three MHWs recorded highest annual number of days in the NZ region for all corresponding annual periods during the satellite-era (1981 - present). Mid-tropospheric (500hPa) atmospheric circulation anomalies were extremely similar with strong blocking to the southeast of NZ. Climate projections with New Zealand's Earth System Model suggest that above average temperature anomalies extending into autumn may become the new normal, as the ocean warms under climate change (Behrens et al., 2022), and the patterns are driven by atmospheric circulation interacting with the oceanic circulation.

Projected circulation changes for the late 21st century (Mullan et al., 2016) show MSLP increases during DJF, especially to the southeast of NZ. The airflow over the country becomes more northeasterly, and at the same time associated with more (possibly blocking) anticyclones and lacking in troughs. There is also a trend towards the positive SAM resulting in higher MSLPs in the NZ region, but this depends on interplay with stratospheric ozone recovery (Arblaster et al., 2011). These are all features displayed in the 2017/18, 2018/19 and 2021/22 heatwaves, with circulation regimes and their analogues exhibiting a lack of the troughing regime. Given that the Tasman Sea mixed layer heat content anomalies are in recent years have been above average, it appears likely that human-induced warming has played a significant role in the three recent coupled ocean-atmospheric heatwaves.

Record-breaking MHWs have been globally documented MHWs (Oliver et al 2021) where the atmospheric state played a central role in their development and maintenance, from the Mediterranean, off the northeast United States and other oceanic areas. In these cases, the anomalously warm ocean temperatures were related to abnormally high air–sea heat fluxes into the ocean, which was the case for the three Tasman Sea/NZ recent MHWs.

Analysis shows that the 1934/35 event was highly unusual with an ERI of over 300 years based on the climate of the time, and of around 40 years even in the climate of the last six decades. However, with 2°C of regional temperature increase all four would be cooler than normal November – March seasons in the future.

All three recent heatwaves produced significant impacts on glaciers and seasonal snow and ice, and on terrestrial and marine ecosystems. Ice loss in small and medium glaciers has been estimated to range from 1.7 to 2.1km^3 w.e. in each event. Across all three heatwave summers, there was an accumulated ice volume loss of 22% of the 2017 volume. In all four cases, SnowSim showed swift snowmelt commencing in mid-November with rapid melt thereafter.

Potential grapevine yield is determined by the number of inflorescence primordia that develop in buds during flowering in the season before harvest, and then the number of berries that set during flowering in the current season (Trought, 2005). Following pollination of the stigma, which occurs shortly after sunrise (Staudt, 1999), pollen tube growth ceases after approximately 18 hours (Staudt, 1982) with the result that the maximum growth of the pollen tube reflects temperatures after pollination, with an estimated mean temperature of 18°C required for fertilization to be successful (Trought, 2005). The low Sauvignon blanc and Pinot noir yields at the 2021 harvest were associated with below average initiation and flowering temperatures of 16.0 and 17.4 respectively, in particular a cold period at the height of flowering in late December. While higher yields in 2022 can be attributed to the initiation and flowering temperatures of 16.8 and 18.9°C respectively.

While the number of spring frosts has declined nationwide since 1948, by approximately 0.19 events per year, and date of the last frost has come forward by a month since 1948, the increase in temperature has advanced the date of budburst and flowering, with the result spring frost risk, the temperature during flowering or ripening has changed little since 1948. Similar changes in frost risk have been observed in Europe (Sgubin et al., 2018). Likewise, mean temperatures during the ripening period did not increase, unlike increases observed elsewhere (Molitor and Junk, 2019). This possibly reflects the temperate climate of Marlborough and the abrupt changes in temperature that may occur between concurrent phenophases of vine development during the season (Salinger et al., 2020).

The slow advances in grapevine phenology since 1948 may be associated with increases in temperature over the same period, marked inter-seasonal variation in temperature, particularly in relation to spring frost, inflorescence initiation and flowering, key stages of yield development, result in marked fluctuation in seasonal yield. Cherries and apricots showed an advancement date for the three AHW warm seasons harvest dates by 12 and 8 days respectively.

The observed impacts of the 2022 marine heatwave on marine sponges in northern NZ and Fiordland are unprecedented and raise concerns for the future of sponge communities which are an important component of temperate reef ecosystems. The contrasting impacts of the marine heatwave on sponges between northern NZ and Fiordland highlight there are multiple mechanisms at play and further research is needed to better understand the actual mechanisms and species-specific vulnerabilities of sponges to marine heatwaves. The longer-term impacts for the sponges that have lost tissue is currently unknown and further monitoring will be needed to assess if they survive or not around northern and southern NZ.

Reduced breeding attempts of kororā, lower chick masses and fewer chicks per pair may be related to increased SST (Cannel et al., 2012; Johnson & Colombelli-Négrel, 2021), but the difference between chicks per pair in this study is marginal and could not be attributed to

Figure 13: One of twelve emaciated kororā found over the 2021/2022 spring/summer period in the Bay of Plenty. A recent fledgling weighing 335g washed ashore weak and dehydrated, on Waihi Beach during the marine heatwave, January 2022.

Figure 14: A group of bleached *Cymbastella lamellata* from Dusky Sound, Fiordland. These sponges contain photosynthetic symbionts and are normally brown in colour. During the 2022 marine heat wave these symbionts were lost from these sponges. Over 90% of sponges across the entire Fiorldand Marine Area were bleached.

ocean conditions. An increase in non-breeding birds could indicate adults sheltering during the day, birds pairing and/or lack of food availability resulting in reduced breeding attempts. Similarly, developmental delays in kororā chicks have also been observed in malnourished chicks going into rehabilitation in Tasmania (Grieveson, pers. comm). Starvation could likely be linked to reduced prey capture success during periods of increased SST (Carroll et al., 2016) that occurred in the Northern North Island resulting in increased hotline call volumes and emaciated kororā washing ashore in the Bay of Plenty, however due to limitations of methodology it cannot be accurately concluded that starvation was the primary cause of death. Disruption to marine ecosystems during 2010/2011 has been previously linked to a significant marine heatwave in Western Australia (Salinger et al., 2016) including an increased number of dead kororā found washed ashore that had died of starvation (Caputi et al., 2014). Hocken (2000) found starvation as the leading cause of mortality in kororā washed ashore in Otago during 1994 to 1998. One of the primary concerns of increased ocean temperatures is the decrease in adult survival, particularly if high numbers of emaciated fledglings are seen and low juvenile recruitment continues. A population model demonstrated a 9% decrease in survival of adult king penguins for a 0.26°C warming in the Southern Ocean (Le Bohec et al., 2008). It is likely that other environmental variables, such as increased wind speeds and high land temperatures (Johnson and Colombelli-Négrel, 2021; Stahel and Gales, 1987) were also contributing factors in reduced breeding success and starvation and requires further investigation. Little is known about the prey species of the Mount Maunganui kororā colony. Further research is needed to investigate the diet of kororā in the Bay of Plenty to find out whether not just sea temperature but also dredging and fishing activities impact breeding success and survival.

The only records of pilchard and/or anchovy in the diet of yellow-eyed penguin at Moeraki through eight years beginning in 2014 was during the last year. Monitoring of the diet of this penguin is ongoing and will document whether or not pilchard and/or anchovy gradually become important in the diet indicating prey switching attributable a southward spread of these small pelagic fishes in response to warming sea temperatures.

ACKNOWLEDGEMENTS

Updates of the Tasman Glacier end of summer snow line data to 1976 were provided by the late Dr Trevor Chinn. Other files from Trevor were used to update the proglacial lake and downwasting of volume for the 12 large glaciers. Pascal Sirguey provided mass balance information from the Brewster Glacier. The Argo data were collected and made freely available by the International Argo Program and the national programs that contribute to it (http://www.argo.ucsd.edu, http://argo.jcommops.org).

The Argo Program is part of the Global Ocean Observing System. The sub-surface temperature and SST data was collected as part of the MBIE funded Coastal Acidification: Rate, Impacts and Management (CARIM) project, provided by Kim Currie. This project obtained support through the Deep South National Science Challenge. This paper was supported through funding from the Ministry of Business, Innovation and Employment via the Deep South National Science Challenge (C01X1902). MST was funded by the Brian Mason Trust (Impact of an unprecedented marine heatwave). PMS was funded by MBIE contract CAWX1801. Bay of Plenty kororā research was obtained under wildlife authorities (48462-FAU & 81642-DOA), thanks to the Department of Conservation, local iwi (Ngai Te Rangi, Ngati Ranginui and Ngati Pukenga) and Tauranga City Council for granting permissions and land use access.

REFERENCES

Arblaster, J.M., Meehl, G.A., & Karoly, D.J. 2011. Future climate change in the Southern Hemisphere: Competing effects of ozone and greenhouse gases. *Geophysical Research Letters*, 38(2). https://doi.org/10.1029/2010GL045384

Bell, J.J., Smith, R.O., Micaroni, V., Strano F., Balemi, C.A., Caiger, P.E., Miller, K.I., Spyksma, A.J.P., & Shears, N.T. 2022. Marine heat waves drives bleaching and necrosis of temperate sponges. *Current Biology,* https://doi.org/10.1016/j.cub.2022.11.013

Behrens, E., Fernandez, D., & Sutton, P 2019. Meridional Oceanic Heat Transport Influences Marine Heatwaves in the Tasman Sea on Interannual to Decadal Timescales. *Frontiers Marine Science*, 6: 228. https://doi.org/10.3389/fmars.2019.00228

Behrens, E., Hogg, A. M., England, M. H., & Bostock, H. 2021. Seasonal and interannual variability of the subtropical front in the New Zealand Region. *Journal of Geophysical Research: Oceans*, 126, e2020JC016412. https://doi.org/10.1029/2020JC016412.

Behrens, E., Rickard, G., Rosier, S., Williams, J., Morgenstern, O., & Stone, D. 2022. Projections of future marine heatwaves for the Oceans Around New Zealand Using New Zealand's Earth System Model. *Frontiers in Climate*, 4: 798287. https://doi.org/10.3389/fclim.2022.798287.

Blunden, J. & T. Boyer, Eds. 2020. State of the Climate in 2020. *Bulletin of the American Meteorological Society*, 102 (8): Si–S475, https://doi:10.1175/2021BAMSStateoftheClimate.1.

Cannell, B., Chambers, L., Bunce, M. & Murray, D. 2012. *Little Penguins (Eudyptula minor) breeding and survival in Western Australia compromised by a "marine heat wave" in 2011*. In: Abstracts of the Australian Marine Sciences Association and New Zealand Marine Sciences Society Joint Conference, 1 - 5 July, Hobart, Tasmania.

Caputi, N, Jackson, G, and Pearce, A. (2014). *The marine heat wave off Western Australia during the summer of 2010/11 – 2 years on*. Government of Western Australia Department of Fisheries, Perth. Report Fisheries Research Report No. 250.

Carroll, G., Everett, J. D., Harcourt, R., Slip, D., & Jonsen, I. 2016. High sea surface temperatures driven by a strengthening current reduce foraging success by penguins. *Scientific Reports*, 6(1). https://doi.org/10.1038/srep22236.

Chinn, T.J. 2001. Distribution of the glacial water resources of New Zealand. *Journal of Hydrology New Zealand*, 40 (2): 139–187. https://www.jstor.org/stable/43922047.

Chinn, T.J., Fitzharris, B.B., Salinger, M.J, & Willsman, A. 2012. Annual ice volume changes 1976–2008 for the New Zealand Southern Alps. *Global and Planetary Change*, 92-93: 105-118. https://doi.org/10.1016/j.gloplacha.2012.04.002.

Chiswell, S.M. & Sutton, P.J. 2020. Relationships between long-term ocean warming, marine heat waves and primary production in the New Zealand region. *New Zealand Journal of Marine and Freshwater Research*, 54(4): 614-635.

Compo, G. P., J. S. Whitaker, P. D. Sardeshmukh, N. Matsui, R. J. Allan, X. Yin, B. E. Gleason, R. S. Vose, G. Rutledge, P. Bessemoulin, S. Brönnimann, M. Brunet, R. I. Crouthamel, A. N. Grant, P. D. Jones, M. C. Kruk, A. C. Kruger, G. J. Marshall, M. Maugeri, H. Y. Mok, Ø. Nordli, T. F. Ross, R. M. Trigo, X. L. Wang, S. D. Woodruff, and S. J. Worley, 2011. The Twentieth Century Reanalysis Project, *Quarterly Journal of the Royal Meteorological Society*, 137 (654), 1-28, doi: https://doi.org/10.1002/qj.776

Dee, D.P., Uppala, S.M., Simmons, A.J., Berrisford, P., Poli, P., Kobayashi, S., et al & Vitart, F. 2011. The ERA-Interim reanalysis: configuration and performance of the data assimilation system. *Quarterly Journal of the Royal Meteorological Society*, 137(656): 553-597. https://doi.org/10.1002/qj.828.

de Lautour, S. 1999. *The climatology of seasonal snow*. MSc Thesis, Department of Geography, University of Otago.

Department of Conservation 2022. *Marine Monitoring and Reporting Framework*. ISBN: 978-1-99-116198-7.

Fitzharris, B., & Garr, G.E. 1995. Simulation of past variability in seasonal snow in the Southern Alps, New Zealand. *Annals of Glaciology*, 21: 377-382. https://doi.org/10.3189/S0260305500016098.

Fogt, R.L., Perlwitz, J., Monaghan, A.J., Bromwich, D.H., Jones, J.M., & Marshall, G.J. 2009. Historical SAM variability. Part II: Twentieth-century variability and trends from reconstructions, observations, and the IPCC AR4 models. *Journal of Climate*, 22, 5346-5365. https://doi.org/10.1175/2009JCLI2786.1.

García De Cortázar-Atauri, I., Brisson, N. & Gaudillere, J. P. 2009. Performance of several models for predicting budburst date of grapevine (Vitis vinifera L.). *International Journal of Biometeorology*, 53(4): 317-326.

Garr, C.E., & Fitzharris, B.B. 1996. Using seasonal snow to forecast inflows into South Island hydro lakes. In: *Prospects and Needs for Climate Forecasting*, The Royal Society of New Zealand Miscellaneous Series 34: 63-67 [ISBN 0-908654-61-8].

Heidemann, H., & Ribbe, J. (2019). Marine Heat Waves and the Influence of El Niño off Southeast Queensland, Australia, *Frontiers of Marine Science*, 20 February 2019. https://doi.org/10.3389/fmars.2019.0005.

Henley, B.J., Gergis, J., Karoly, D.J., Power, S.B., Kennedy, J., & Folland, C.K. 2015. A Tripole Index for the Interdecadal Pacific Oscillation. *Climate Dynamics*, 45 (11-12): 3077-3090. http://dx.doi.org/10.1007/s00382-015-2525-1. Accessed on 05 27 2019 at https://www.esrl.noaa.gov/psd/data/timeseries/IPOTPI.

Hill, M., Walter, C. & Bartels, E. 2016. A mass bleaching event involving clionaid sponges. *Coral Reefs*, 35 (1): 153-153.

Hobday, A., Alexander, L.V., Perkins, S.E., Smale, D.A., Straub, S.C., Oliver, E.C.J., Benthuysen, J.A., Burrows, M.T., Donat, M.G., Feng, M., Holbrook, N.J., Moore, P.J., Scannell, H.A., Sen Gupta, A., & Wernberg, T. 2016. A hierarchical approach to defining marine heatwaves. *Progress in Oceanography* 141: 227–238. https://doi.org/10.1016/j.pocean.2015.1012.1014. Outcome of Workshop #1.

Hobday, A.J., E.C.J. Oliver, A. Sen Gupta, J.A. Benthuysen, M.T. Burrows, M.G. Donat, N.J. Holbrook, P.J. Moore, M.S. Thomsen, T. Wernberg, & Smale., D.A. 2018. Categorizing and naming marine heatwaves. *Oceanography,* 31(2): 162–173, https://doi.org/10.5670/oceanog.2018.205.

Hocken, A. G. 2000. Cause of death in blue penguins (Eudyptula m. minor) in North Otago, New Zealand. *New Zealand Journal of Zoology*, 27(4): 305–309. https://doi.org/10.1080/03014223.2000.9518239.

Huang, B., Thorne, P. W., Banzon, V. F., Boyer, T., Chepurin, G., Lawrimore, J. H., & Zhang, H.-M. 2017. Extended Reconstructed Sea Surface Temperature, Version 5 (ERSSTv5): Upgrades, Validations, and Intercomparisons. *Journal of Climate*, 30 (20): 8179-8205. https://doi.org/10.1175/jcli-d-16-0836.1.

Huang, B., Liu, C., Banzon, V., Freeman, E., Graham, G., Hankins, B., Smith, T., & H.-M. 2020. Improvements of the Daily Optimum Interpolation Sea Surface Temperature (DOISST) Version 2.1, *Journal of Climate*, 34: 2923-2939. https://doi.org/10.1175/JCLI-D-20-0166.1.

Jayne, S.R., Roemmich, D., Zilberman, N., Riser, S.C., Johnson, K.S., Johnson, K.C., & Piotrowicz, S.R. 2017. The Argo Program: present and future, *Oceanography,* 30: 18–28. https://doi.org/10.5670/oceanog.2017.213

Johnson, B., & Colombelli-Négrel, D. 2021. Breeding success in Southern Australian Little Penguins is negatively correlated with high wind speeds and sea surface temperatures. *Ornithological Applications,* 123(2021): 1-15. https://doi.org/10.1093/ornithapp/duaa062.

Kanamitsu, M., W. Ebisuzaki, J. Woollen, S-K Yang, J.J. Hnilo, M. Fiorino, and G. L. Potter, 2002. NCEP-DOE AMIP-II Reanalysis (R-2): *Bulletin of the American Meteorological Society*, 83(11), 1631-1643, doi: https://doi.org/10.1175/BAMS-83-11-1631 .

Kidson, E. 1935. The summer of 1934/35 in *New Zealand. New Zealand Meteorological Office Note*, 16: 1- 12.

Kidson, J.W. 2000. An analysis of New Zealand synoptic types and their use in defining weather regimes. *International Journal of Climatology*, 20 (3): 299-315. https://doi.org/10.1002/(SICI)1097-0088(20000315)20:3<299::AID-JOC474>3.0.CO;2-B

Kistler, R., Collins, W., Saha, S., White, G., Woollen, J., Kalnay, E., . . . & Fiorino M. 2001. The NCEP–NCAR 50–year reanalysis: Monthly means CD–ROM and documentation. *Bulletin of the American Meteorological Society,* 82(2): 247–268. https://doi.org/10.1175/1520-0477(2001)082<0247:TNNYRM>2.3.CO;2.

Le Bohec, C., Durant, J. M., Gauthier-Clerc, M., Stenseth, N. C., Park, Y. H., Pradel, R.,Grémillet, D., Gendner, J. P., & le Maho, Y. 2008. King penguin population threatened by Southern Ocean warming. *Proceedings of the National Academy of Sciences*, 105(7): 2493–2497. https://doi.org/10.1073/pnas.0712031105.

López-Legentil, S., Song, B., Mcmurray, S.E. & Pawlik, J.R., 2008. Bleaching and stress in coral reef ecosystems: hsp70 expression by the giant barrel sponge *Xestospongia muta*. *Molecular Ecology*, 17(7): 1840-1849.

MacLean, H. 2019. Seabirds swarm as shoals of fish beach. *Otago Daily Times* 12 December 2019. https://www.odt.co.nz/regions/north-otago/seabirds-swarm-shoals-fish-beach.

McLuskie, M. (2023). *Kororā/Little Blue Penguin Project: Current Trends and Key Threats*. Western Bay Wildlife Trust (Mount Maunganui Little Blue Penguin (*Eudyptula minor*) Colony (westernbaywildlife.nz)).

McMillan, P.J, Francis, M.P, James, G.D, Paul, L.J, Marriott, P, Mackay, E, Wood, B.A, Stevens, D.W, Griggs, L.H, Baird, S.J, Roberts, C.D, Stewart, A.L, Struthers, C.D & Robbins, J.E. 2019. *New Zealand fishes. A field guide to common species caught by bottom, midwater, and surface fishing*. New Zealand Aquatic Environment and Biodiversity Report No. 208.

McMurray, S.E., Blum, J.E., Leichter, J.J. & Pawlik, J.R., 2011. Bleaching of the giant barrel sponge *Xestospongia muta* in the Florida Keys. *Limnology and Oceanography*, 56(6): 2243-2250.

Madec, G., Bourdallé-Badie, R., Bouttier, P. A., Bricaud, C., Bruciaferri, D., Calvert, D., et al. 2017. *NEMO Ocean Engine.*

Marlow, J., Davy, S.K., Shaffer, M., Haris, A. & Bell, J.J., 2018. Bleaching and recovery of a phototrophic bioeroding sponge. *Coral Reefs,* 37(2): 565-570.

Marshall, G.J. 2003. Trends in the southern annular mode from observations and reanalyses. *Journal of Climate*, 16: 4134–4143. https://doi.org/10.1175/1520-0442(2003)016<4134:TITSAM>2.0.CO;2.

Ministry for the Environment & Stats NZ 2019. New Zealand's Environmental Reporting Series: *Environment Aotearoa 2019*. https://environment.govt.nz/assets/Publications/Files/environment-aotearoa-2019.pdf.

Molitor, D., & Junk, J. 2019. Climate change is implicating a two-fold impact on air temperature increase in the ripening period under the conditions of the Luxembourgish grapegrowing region. *Oeno-one*. 3: 409-422. https://doi.org/10.20870/oeno-one.2019.53.3.2329.

Mullan, A.B., Stuart, S.J., Hadfield. M.G., Smith, M.J. 2010. *Report on the Review of NIWA's 'Seven-Station' Temperature Series* NIWA Information Series No. 78. 175 pp. https://www.niwa.co.nz/sites/niwa.co.nz/files/import/attachments/Report-on-the-Review-of-NIWAas-Seven-Station-Temperature-Series_v3.pdf.

Mullan, A.B., Sood, A., Stuart, S. 2016. *Climate Change Projections for New Zealand: Atmosphere Projections Based on Simulations from the IPCC Fifth Assessment*, Wellington: Ministry for the Environment. https://www.mfe.govt.nz/sites/default/files/media/Climate%20Change/Climate-change-projections-2nd-edition-final.pdf.

Oliver, E.C.J., Benthuysen, J.A., Bindoff, N.L., Hobday, A.J., Holbrook, N.J., Mundy, C.N., & Perkins-Kirkpatrick, S.E. 2017. The unprecedented 2015/16 Tasman Sea marine heatwave. *Nature Communications*, 8: 16101 https://doi.org/10.1038/ncomms16101.

Oliver, E. C., Benthuysen, J. A., Darmaraki, S., Donat, M. G., Hobday, A. J., Holbrook, N. J., et al. 2021. Marine heatwaves. *Annual Review of Marine Science*. 13: 313–342. https://doi.org/10.1146/annurev-marine-032720-095144.

Oliver, E.C.J., Donat, M.G., Moore, P.J., Smale, D.A., Alexander, L.V., Benthuysen, J.A., Feng, M., Gupta, A.S., Hobday, A.J., Holbrook, N.J., PerkinsKirkpatrick, S.E., Straub, S.C., & Wernberg, T. 2018. Longer and more frequent marine heatwaves over the past century. *Nature Communications,* 9: 1324 https://doi.org/10.1038/s41467-018-03732-9.

Parker, A., Garcia de Cortazar-Atauri, I., Chuine, I., Barbeau, G., Bois, B., Boursiquot, J-M., Cahurel, J-Y., Claverie, M., Dufourcq, T., Geny, L., Guimberteau, G., Hofmann, R.W., Jacquet, O., Lacombe, T., Monamy, C., Ojeda, H., Panigai, L., Payan, J-C., Lovelle, B.R., Rouchaud, E., Schneider, C., Spring, J-L., Storchi, P., Tomasi, D., Trambouze, W., Trought, M. & van Leeuwen, C. 2013. Classification of varieties for their timing of flowering and véraison using a modelling approach: A case study for the grapevine species *Vitis vinifera L. Agricultural and*

Forest Meteorology, 180: 249-264. http://dx.doi.org/10.1016/j.agrformet.2013.06.005.

Parker, A.K. 2012. Modelling phenology and maturation of the grapevine *Vitis vinifera* L.: *Varietal differences and the role of leaf area to fruit weight ratio manipulations* Lincoln University PhD thesis, Lincoln University.

Parliamentary Commission for the Environment 2019. *Focusing Aotearoa New Zealand's environmental reporting system*. ISBN 978-0-947517-17-5

Perkins, N.R., Monk, J., Soler, G., Gallagher, P. & Barrett, N.S 2022. Bleaching in sponges on temperate mesophotic reefs observed following marine heatwave events. Climate Change Ecology, 3: 100046.

Perkins-Kirkpatrick, S.E., King, S.E., Cougnon, A.D., Grosese, E.A., Oliver, M.R., Holbrook, N.J., Lewis, S.C., & Pourasghar, F 2019. The role of natural variability and anthropogenic climate change in the 2017/18 Tasman Sea marine heatwave. *Bulletin of American Meteorological Society,* 100: S105-110 http://doi.org/10.1175/BAMS-D-18-0116.1.

Ratz, H. (2022). Pers. comm.

Roberts, C., Stewart, A.L., & Struthers, C. D. 2015. *The fishes of New Zealand*. Wellington, Te Papa Press, 2008 pp.

Saha, S. et al 2006. The NCEP climate forecast system. *Journal of Climate* 19: 3483–3517. https://doi.org/10.1175/JCLI-D-12-00823.1.

Salinger, M. J. 1979. New Zealand climate: the temperature record, historical data and some agricultural implications. *Climatic Change*, 2: 109-126. https://doi.org/10.1007/BF00133218.

Salinger, M.J., Diamond, H.J., & Renwick, J.A. 2020. Surface temperature trends in New Zealand and surrounding oceans 1870 – 2019. *Weather and Climate*, 40: 32-50.

Salinger, M.J., McGann, R.P., Coutts, L., Collen, B., & Fouhy, E. (1992). *South Pacific historical climate network. Temperature trends in New Zealand and outlying islands*, 1920-1990. New Zealand Meteorological Service, 46pp, Wellington. ISBN 0-477-01598-0.

Salinger, M.J., Diamond, H.J., Behrens, E., Fernandez, D., Fitzharris, B.B., Herold, N., Johnstone, P., Kerckhoffs, H., Mullan, A.B., Parker, A.K., Renwick, J.A., Schofield, C., Siano, A., Smith, R.O., South, P., Sutton, P.J. Teixeira E., Thomsen, M.S, & Trought, M.C.T. 2020. Unparalleled coupled ocean/atmosphere summer heatwaves in the New Zealand region: Drivers, mechanisms and impacts. *Climatic Change*, 162: 485–506. https://doi.org/10.1007/s10584-020-02730-5.

Salinger, J., Hobday, A.J., Matear, R.J., O'Kane, T.J., Risbey, J.S., Dunstan, P., Eveson, J.P., Fulton, E.A., Feng, M., Plagányi, É.E., Poloczanska, E.S., Marshall, A.G. and Thompson, P.A. 2016. Decadal-Scale Forecasting of Climate Drivers for Marine Applications. *Advances in Marine Biology* 74: 1-68. https://doi.org/10.1016/bs.amb.2016.04.002

Salinger, M.J., Renwick, J.A., Behrens, E., Mullan, A.B., Diamond, H.J., Sirguey, P., Smith, R.O., Trought, M.C.T., Alexander, L.V., Cullen, N.C., Fitzharris, B.B., Hepburn, C.D., Parker, A.K., & Sutton, P.J. 2019a. The unprecedented coupled ocean-atmosphere summer heatwave in the New Zealand region 2017/18: Drivers, mechanisms and impacts. *Environmental Research Letters*, 14 (4). https://doi.org/10.1088/1748-9326/ab012a.

Salinger, M.J., Fitzharris, B., Chinn, T., & Willsman, A. 2019b. Climate forcing of glacier volume change in the Southern Alps of New Zealand, *International Journal of Climatology*, 39(11): 4274-4287. https://doi.org/10.1002/joc.6072.

Salinger, M. J., Fitzharris, B. B., & Chinn, T. 2021. Extending end-of-summer-snowlines for the Southern Alps glaciers of New Zealand back to 1949 (2021). *International Journal of Climatology*, 41 (13):, 6122-6132. https://doi.org/10.1002/joc.7177.

Seneviratne, S.I., Zhang, Adnan, M., Baldi, W., Dereczynski, C., Di Luca, A., Ghosh, S., Iskandar, I., Kossin, J., Lewis, S., Otto, F., Pinto, I., Satoh, M., Vicente-Serrano, S.M., Wehner, M., & B. Zhou, 2021: Weather and Climate Extreme Events in a Changing Climate. In *Climate Change 2021: The Physical Science Basis. Contribution of Working Group I to the Sixth Assessment Report of the Intergovernmental Panel on Climate Change*, edited by Masson-Delmotte, V., P. Zhai, A. Pirani, S.L. Connors, C. Péan, S. Berger, N. Caud, Y. Chen, L. Goldfarb, M.I. Gomis, M. Huang, K. Leitzell, E. Lonnoy, J.B.R. Matthews, T.K. Maycock, T. Waterfield, O. Yelekçi, R. Yu, & B. Zhou. Cambridge, United Kingdom and New York, Cambridge University Press: 1513–1766, https://doi.org/10.1017/9781009157896.013.

Smale, D.A., Wernberg, T., Oliver, E.C.J., Thomsen, M., Harvey, B.P., Straub, S.C., Burrows, M.T., Alexander, L.V., Benthusen, J.A., Donat, M, Feng M, PerkinsKirkpatrick, S.E., Scannell, H.A., Sen Gupta, A., Payne, B.L., & Moore, P.J. 2019. Marine heatwaves threaten global biodiversity and the provision of ecosystem services. *Nature Climate Change*, 9: 306–312 https://doi.org/10.1038/s41558-019-0412-1.

Srinivasan, R., Carey-Smith, T., & Macara, G. 2021. Trend analysis on frequency of New Zealand climate extremes. *Weather and Climate*, 41 (1): 18-29.

Stahel, C & Gales, R. 1991. *Little penguins: fairy penguins in Australia*. University if New South Wales, Kensington, NSW: 115 pp.

Staudt, G. 199). Opening of flowers and time of anthesis in grapevines, *Vitis vinifera*, L. Vitis 38(1): 15-20.

Storkey, D., Blaker, A. T., Mathiot, P., Megann, A., Aksenov, Y., Blockley, E. W., Calvert, D., Graham, T., Hewitt, H. T., Hyder, P., Kuhlbrodt, T., Rae, J. G. L., & Sinha, B. 2018. UK Global Ocean GO6 and GO7: a traceable hierarchy of model resolutions, *Geoscientific Model Development*, 11: 3187–3213, https://doi.org/10.5194/gmd-11-3187-2018, 2018.

Stevens, C. L., O'Callaghan, J. M., Chiswell, S. M. & Hadfield, M. G. 2021. Physiological oceanography of New Zealand/Aotearoa shelf seas – a review. *New Zealand Journal of Marine and Freshwater Research* 55 (1): 6-45. https://doi.org/10.1080/00288330.2019.1588746.

Sutton, P. J. H. 2003. The Southland Current: a subantarctic current. *New Zealand Journal of Marine and Freshwater Research* 37: 645-652.

Sutton, P.J., Bowen, M. 2019. Ocean temperature change around New Zealand othe last 36 years. *New Zealand Journal of Marine and Freshwater Research* 53 (3): 305-326. https://doi.org/10.1080/00288330.2018.1562945.

Tait, L.W., Thoral, F., Pinkerton, M.H., Thomsen, M.S. and Schiel, D.R., 2021. Loss of giant kelp, Macrocystis pyrifera, driven by marine heatwaves and exacerbated by poor water clarity in New Zealand. *Frontiers in Marine Science*, 8: 1-15. https://doi.org/10.3389/fmars.2021.721087

Thompson, D. W. J., Solomon, S., Kushner, P. J., England, M. H., Grise, K. M., & Karoly, D. J. (2011). Signatures of the Antarctic ozone hole in Southern Hemisphere surface climate change. *Nature Geoscience* 4(11), 741-749. https://doi.org/10.1038/NGEO1296.

Thomsen, M.S., Mondardini, L., Alestra, T., Gerrity, S., Tait, L., South, P.M., Lilley, S.A. and Schiel, D.R., 2019. Local extinction of bull kelp (Durvillaea spp.) due to a marine heatwave. *Frontiers in Marine Science*, 6, p.84. https://doi.org/10.3389/fmars.2019.00084.

Thoral, F., Montie, S., Thomsen, M.S., Tait, L.W., Pinkerton, M.H. and Schiel, D.R., 2022. Unravelling seasonal trends in coastal marine heatwave metrics across global biogeographical realms. *Scientific reports*, 12: 7740. https://doi.org/10.1038/s41598-022-11908-z

Trenberth, K.E. 1976. Fluctuations and trends in indices of the southern hemispheric circulation. *Quarterly Journal of the Royal Meteorological Society*, 102 (431): 65-75. https://doi.org/10.1002/qj.4971024310.

Trenberth, K.E., Zhang, Y., Fasullo, J.T., Cheng, L. 2019. Observation-Based Estimates of Global and Basin Ocean Meridional Heat Transport Time Series. *Journal of Climate*, 32: 4567-4583. https://doi.org/10.1175/JCLI-D-18-0872.1.

Trought, M.C.T. 2005. Fruitset - possible implications on wine quality. In: *Transforming flowers to fruit. Mildura, Australia: Australian Society of Viticulture and Oenology*, edited by Garis, K. D., Dundon, C., Johnstone, R. & Partridge, S., Australian Society of Viticulture and Oenology, Mildura, Australia: 32-36.

Troup, A.J. 1965. The 'southern oscillation'. *Quarterly Journal of the Royal Meteorological Society*, 91 (390): 490-506 https://doi.org/10.1002/qj.49709139009.

Tsujino, H., et al. 2018. JRA-55 based surface dataset for driving ocean–sea-ice models (JRA55-do). *Ocean Modelling*, 130 (October 2018): 79-149. https://doi.org/10.1016/j.ocemod.2018.07.002.

Zhao, Z., & Marim, M. 2019. A MATLAB toolbox to detect and analyze marine heatwaves. *Journal of Open Source Software* 4(33): pp.1124, https://doi.org/10.21105/joss.01124.